Laboratoire d'Astrophysique
Ecole Polytechnique Fédérale de Lausanne
Switzerland

The energy profile of the accretion disk in Q2237+030 from 3 years of VLT spectro-photometric monitoring

Frédéric Courbin

with

A. Eigenbrod, G. Meylan, D. Sluse (EPFL)
E. Agol (University of Washington)
T. Anguita, R. Schmidt, J. Wambsganss (ARI, Heidelberg)

ÉCOLE POLYTECHNIQUE
FÉDÉRALE DE LAUSANNE

Laboratoire d'Astrophysique
Ecole Polytechnique Fédérale de Lausanne
Switzerland

EPFL - LABORATOIRE
D'ASTROPHYSIQUE

http://lastro.epfl.ch

Gravitational lensing: numerous applications

- Light magnification:
    - natural telescope (high z galaxies)
    - MACHOS
    - detection of planets
    - quasar structure
- Cosmology:
    - measurement of H_0
    - mapping dark matter
    - measuring dark energy with weak lensing
    - measuring Ω_m and Ω_Λ with lensing statistics
- Galaxies, groups and clusters
    - size and shape of halos
    - X-ray vs. lensing mass
    - nature of dark matter (bullet cluster)

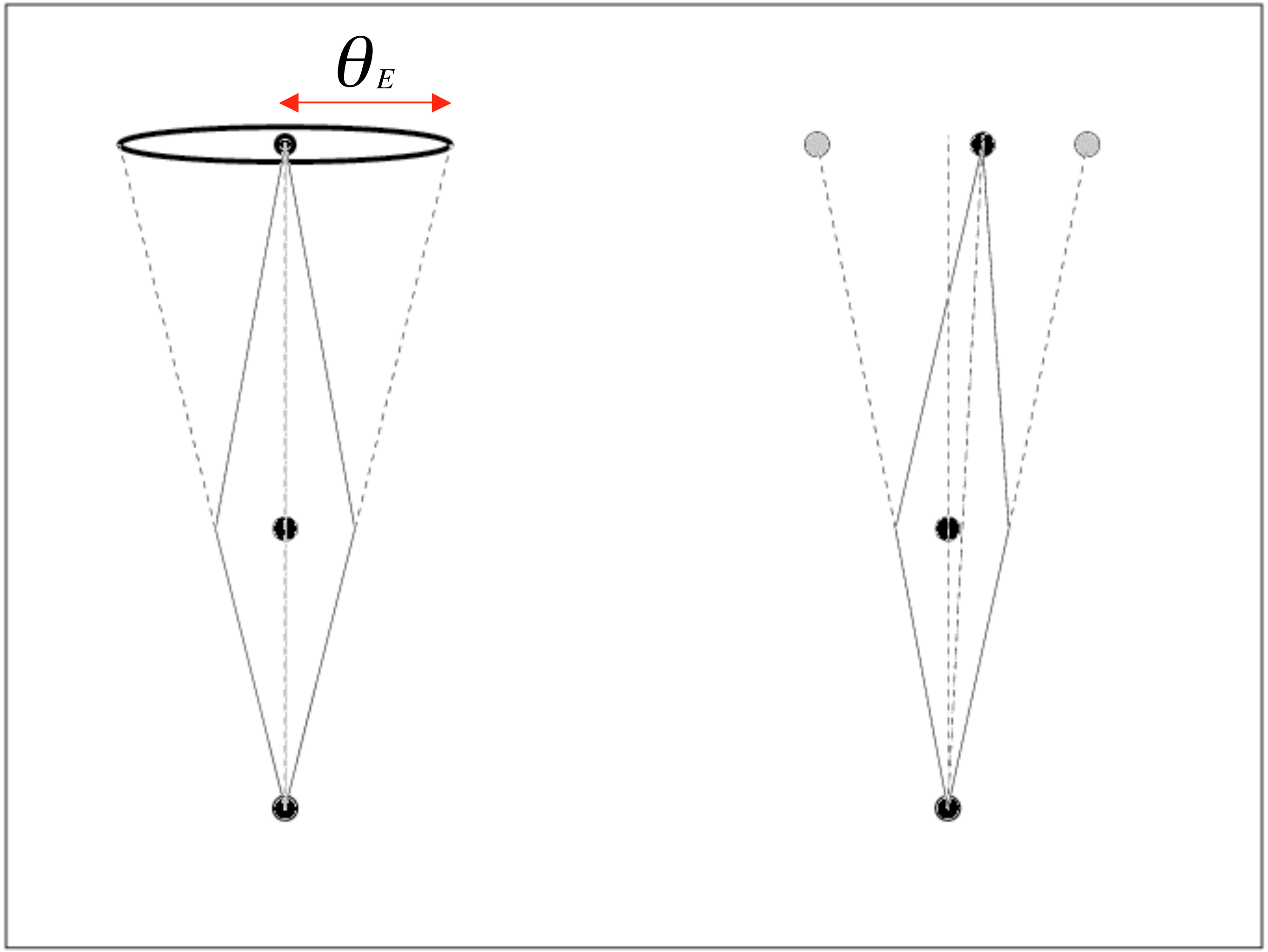

Isothermal sphere

$$\theta_E = 4\pi \frac{\sigma^2}{c^2} \frac{D_{od}}{D_{os}}$$

General mass distribution

$$\theta_E = \sqrt{\frac{4GM}{c^2} \frac{D_{ds}}{D_{od} D_{os}}}.$$

Surface brightness
is conserved

-> magnification

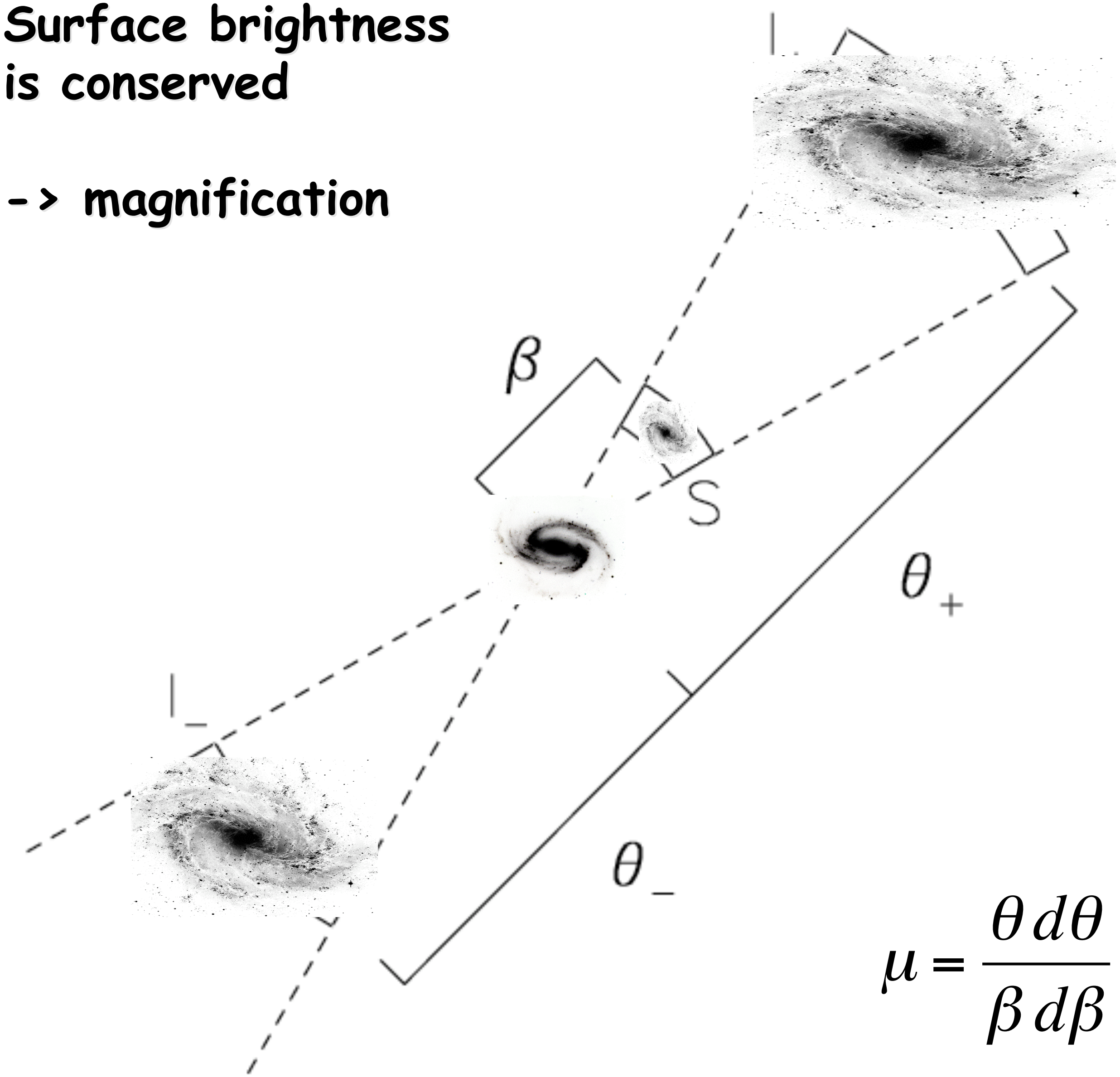

$$\mu = \frac{\theta \, d\theta}{\beta \, d\beta}$$

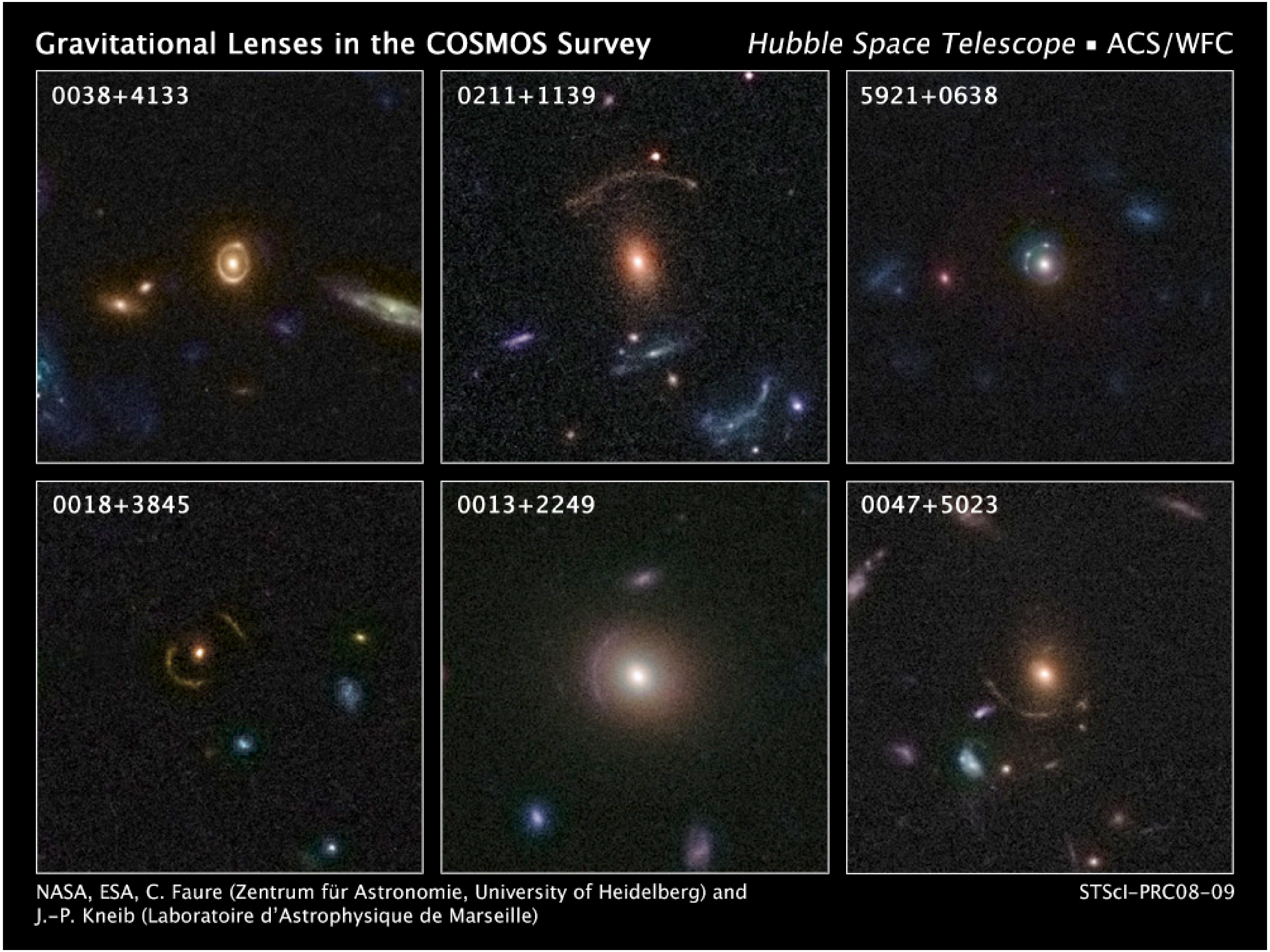
Gravitational Lenses in the COSMOS Survey
Hubble Space Telescope ▪ ACS/WFC
0038+4133
0211+1139
5921+0638
0018+3845
0013+2249
0047+5023
NASA, ESA, C. Faure (Zentrum für Astronomie, University of Heidelberg) and J.-P. Kneib (Laboratoire d'Astrophysique de Marseille)
STScI-PRC08-09

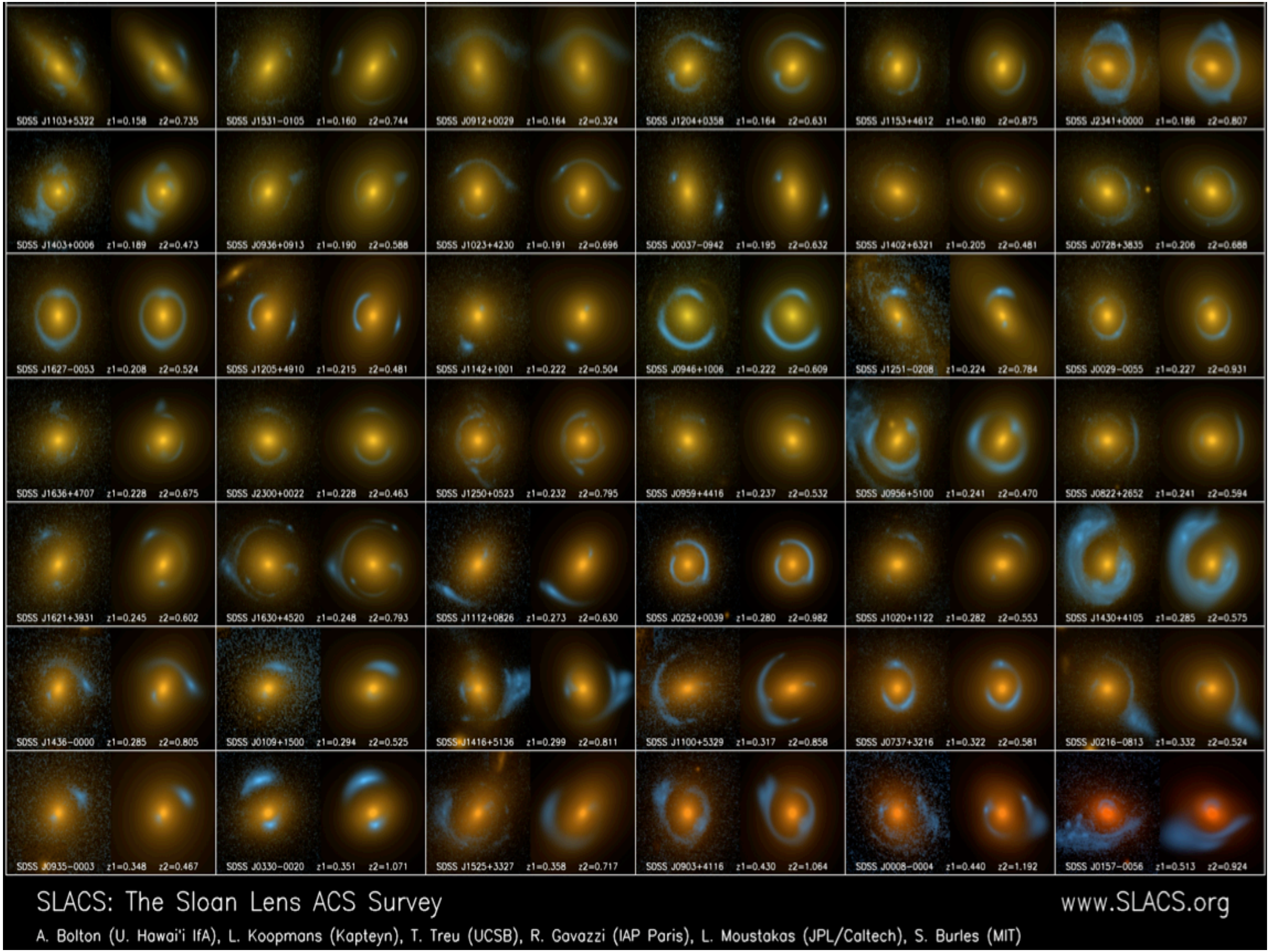
SDSS J1103+5322 z1=0.158 z2=0.735
SDSS J1531-0105 z1=0.160 z2=0.744
SDSS J0912+0029 z1=0.164 z2=0.324
SDSS J1204+0358 z1=0.164 z2=0.631
SDSS J1153+4612 z1=0.180 z2=0.875
SDSS J2341+0000 z1=0.186 z2=0.807
SDSS J1403+0006 z1=0.189 z2=0.473
SDSS J0936+0913 z1=0.190 z2=0.588
SDSS J1023+4230 z1=0.191 z2=0.696
SDSS J0037-0942 z1=0.195 z2=0.632
SDSS J1402+6321 z1=0.205 z2=0.481
SDSS J0728+3835 z1=0.206 z2=0.688
SDSS J1627-0053 z1=0.208 z2=0.524
SDSS J1205+4910 z1=0.215 z2=0.481
SDSS J1142+1001 z1=0.222 z2=0.504
SDSS J0946+1006 z1=0.222 z2=0.609
SDSS J1251-0208 z1=0.224 z2=0.784
SDSS J0029-0055 z1=0.227 z2=0.931
SDSS J1636+4707 z1=0.228 z2=0.675
SDSS J2300+0022 z1=0.228 z2=0.463
SDSS J1250+0523 z1=0.232 z2=0.795
SDSS J0959+4416 z1=0.237 z2=0.532
SDSS J0956+5100 z1=0.241 z2=0.470
SDSS J0822+2652 z1=0.241 z2=0.594
SDSS J1621+3931 z1=0.245 z2=0.602
SDSS J1630+4520 z1=0.248 z2=0.793
SDSS J1112+0826 z1=0.273 z2=0.630
SDSS J0252+0039 z1=0.280 z2=0.982
SDSS J1020+1122 z1=0.282 z2=0.553
SDSS J1430+4105 z1=0.285 z2=0.575
SDSS J1436-0000 z1=0.285 z2=0.805
SDSS J0109+1500 z1=0.294 z2=0.525
SDSS J1416+5136 z1=0.299 z2=0.811
SDSS J1100+5329 z1=0.317 z2=0.858
SDSS J0737+3216 z1=0.322 z2=0.581
SDSS J0216-0813 z1=0.332 z2=0.524
SDSS J0935-0003 z1=0.348 z2=0.467
SDSS J0330-0020 z1=0.351 z2=1.071
SDSS J1525+3327 z1=0.358 z2=0.717
SDSS J0903+4116 z1=0.430 z2=1.064
SDSS J0008-0004 z1=0.440 z2=1.192
SDSS J0157-0056 z1=0.513 z2=0.924
SLACS: The Sloan Lens ACS Survey
www.SLACS.org
A. Bolton (U. Hawai'i IfA), L. Koopmans (Kapteyn), T. Treu (UCSB), R. Gavazzi (IAP Paris), L. Moustakas (JPL/Caltech), S. Burles (MIT)

Double

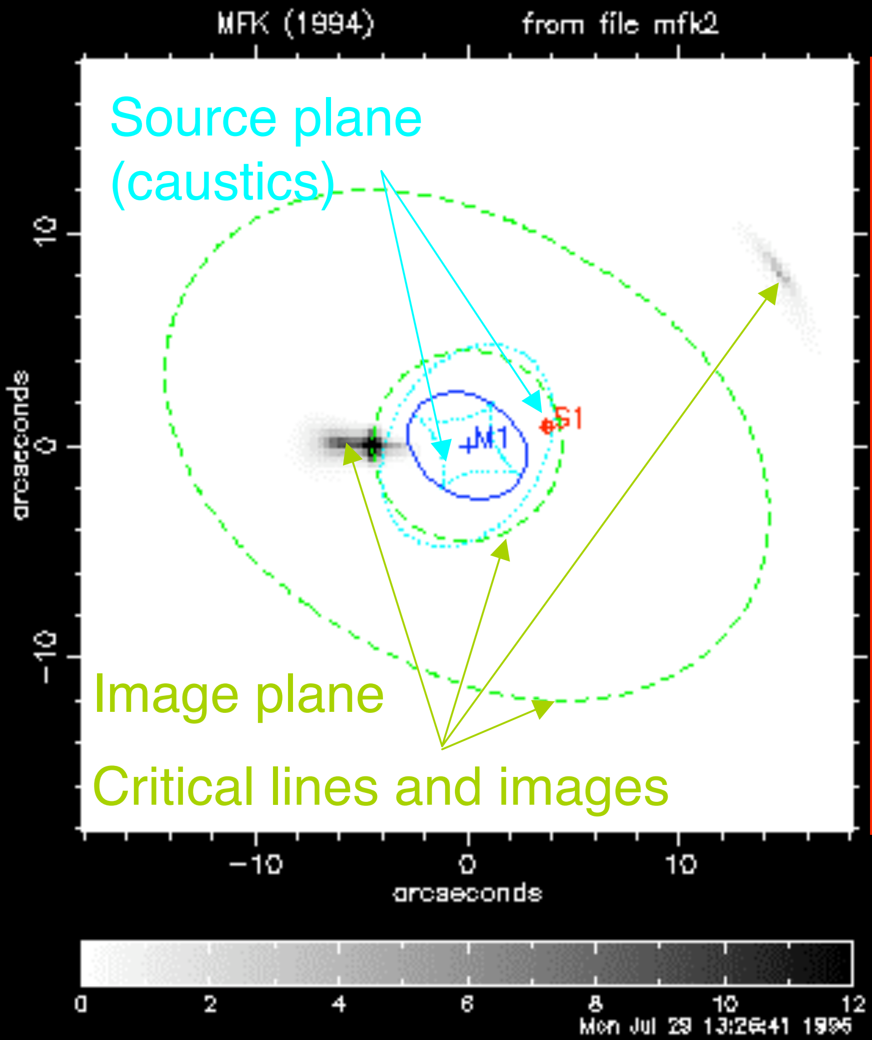
MFK (1994)
from file mfk2
Source plane
(caustics)
Image plane
Critical lines and images
M1
S1
arcseconds
-10
0
10
arcseconds
-10
0
10
0
2
4
6
8
10
12
Mon Jul 29 13:26:41 1996

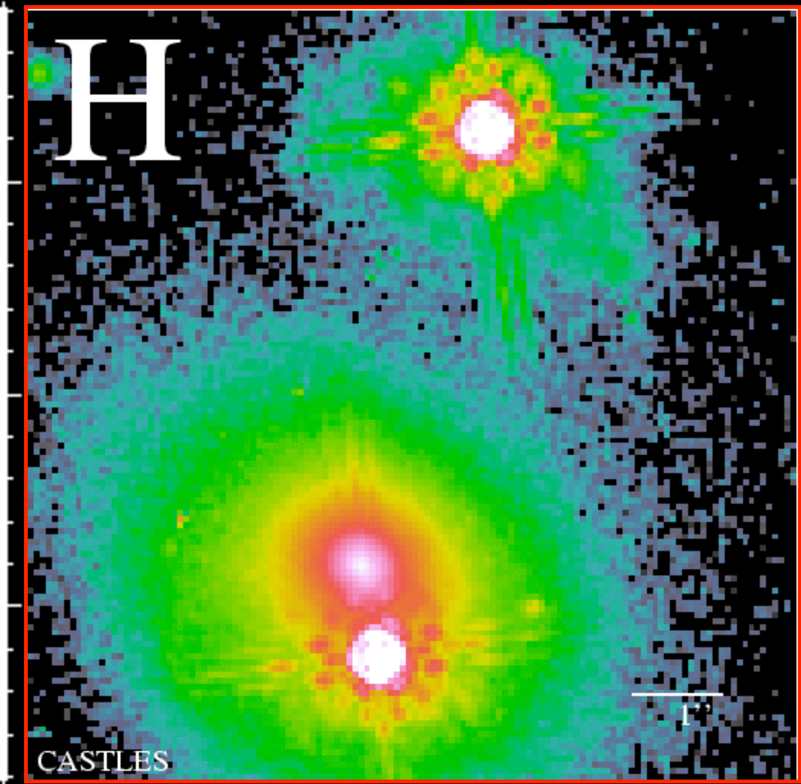
H
1''
CASTLES

Symetric quadruple

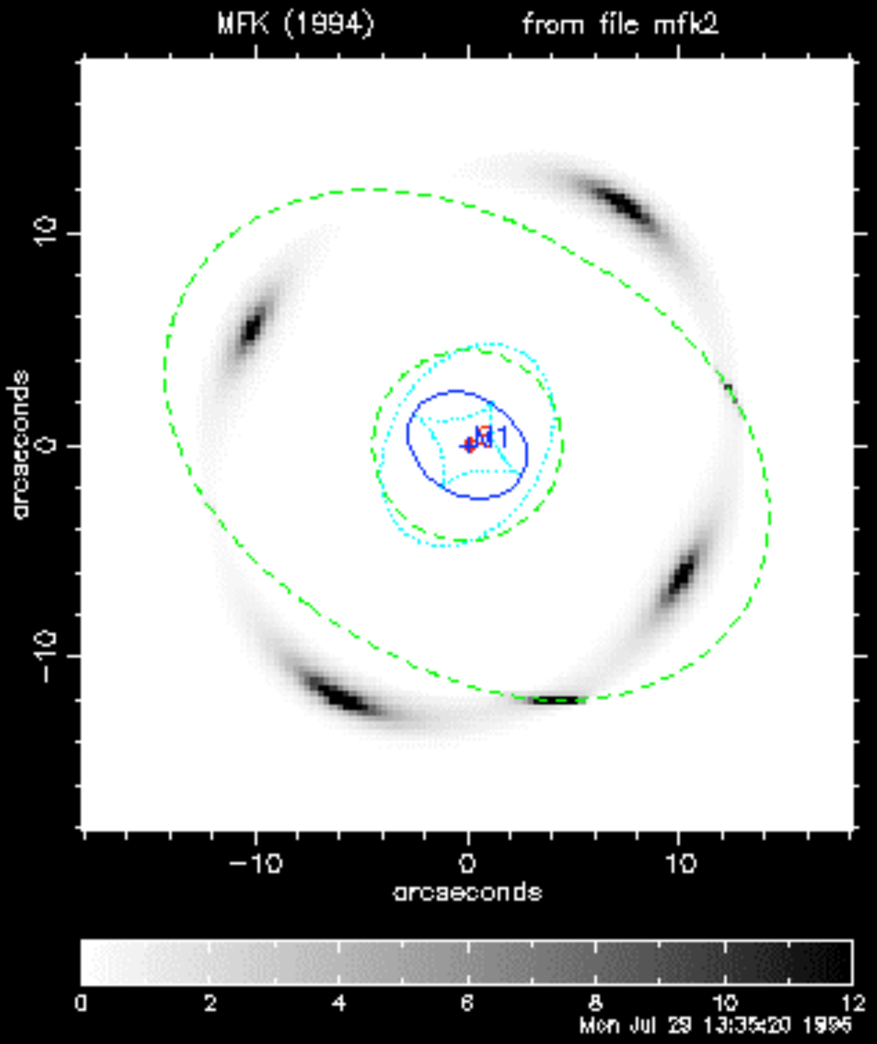

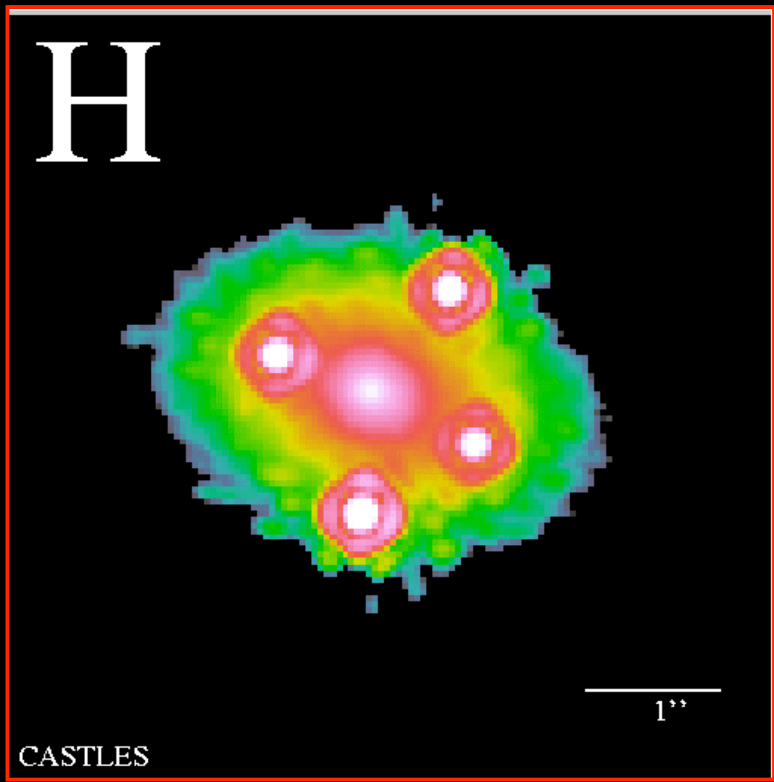

Assymetric quadruple

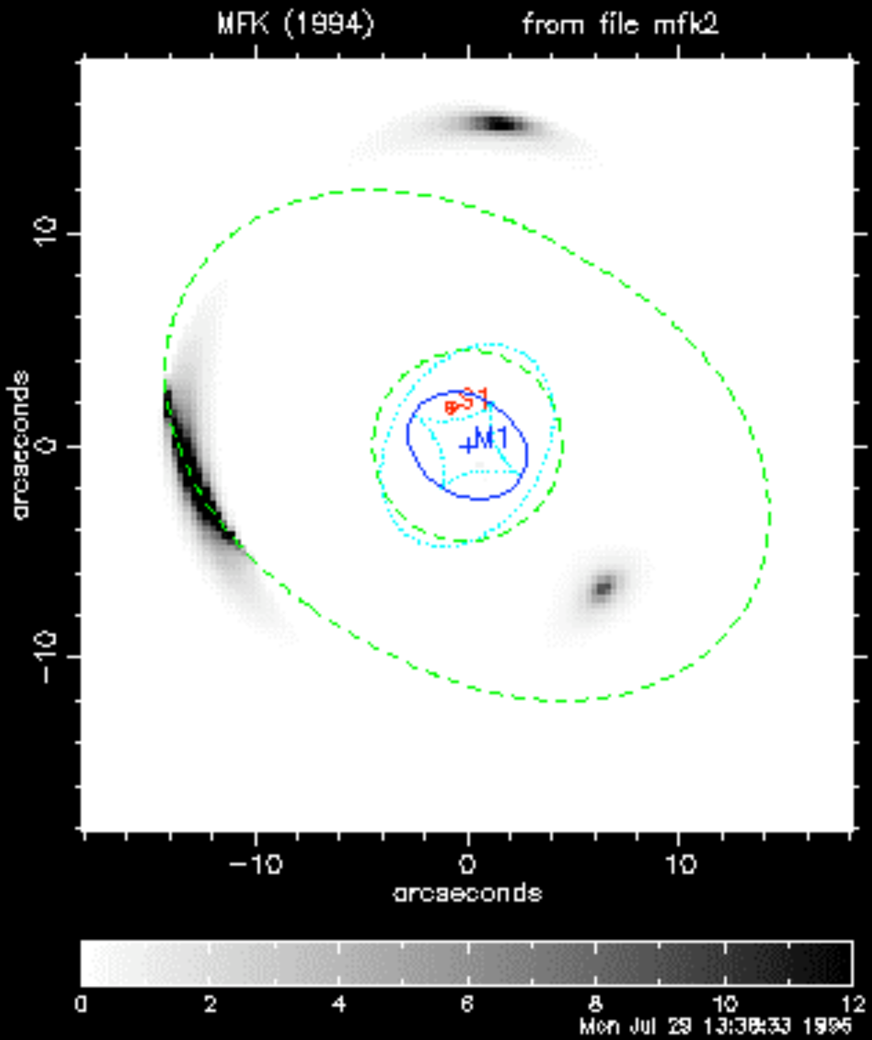

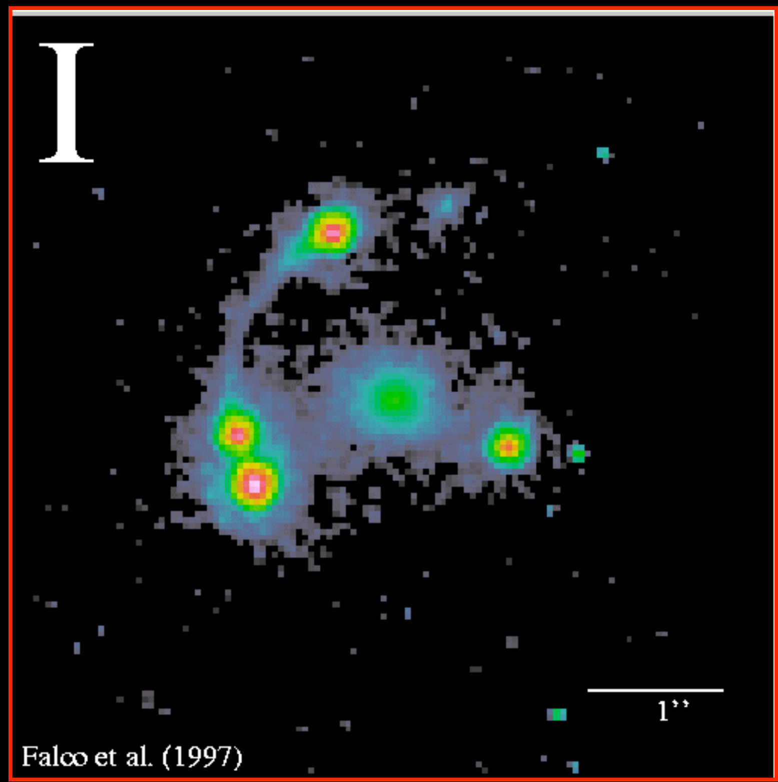

Long axis quadruple

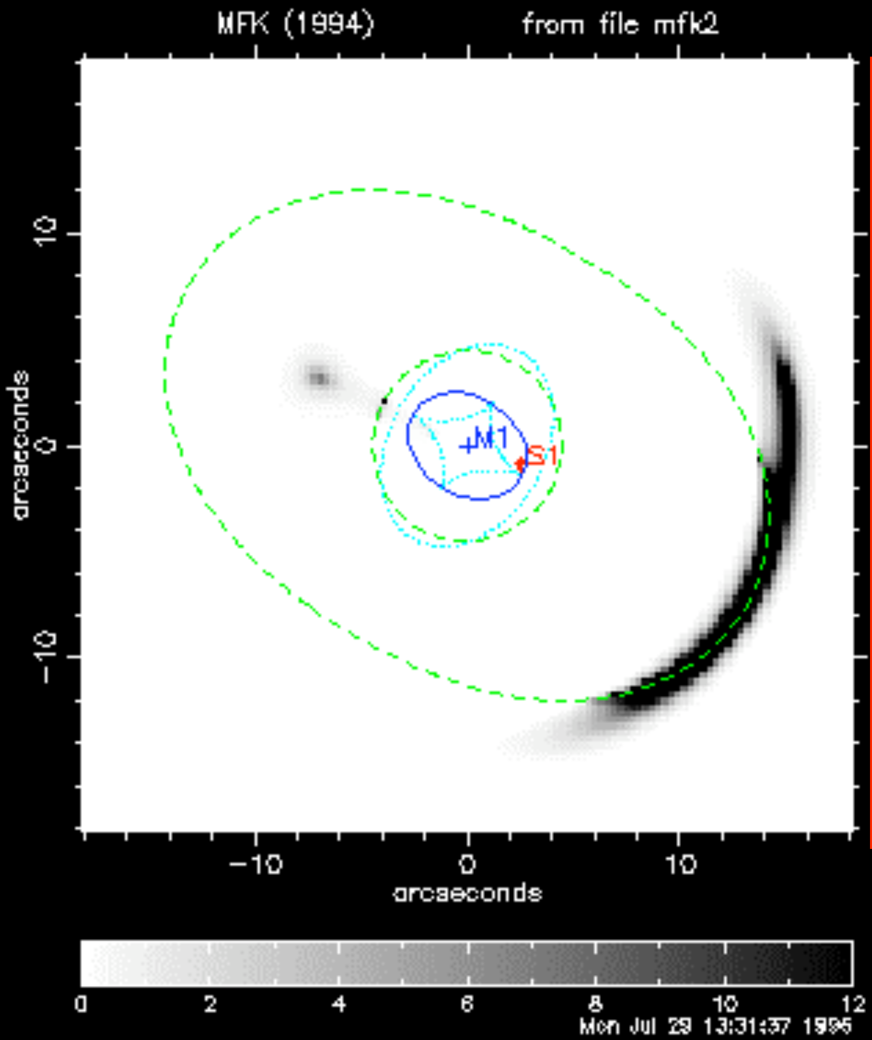

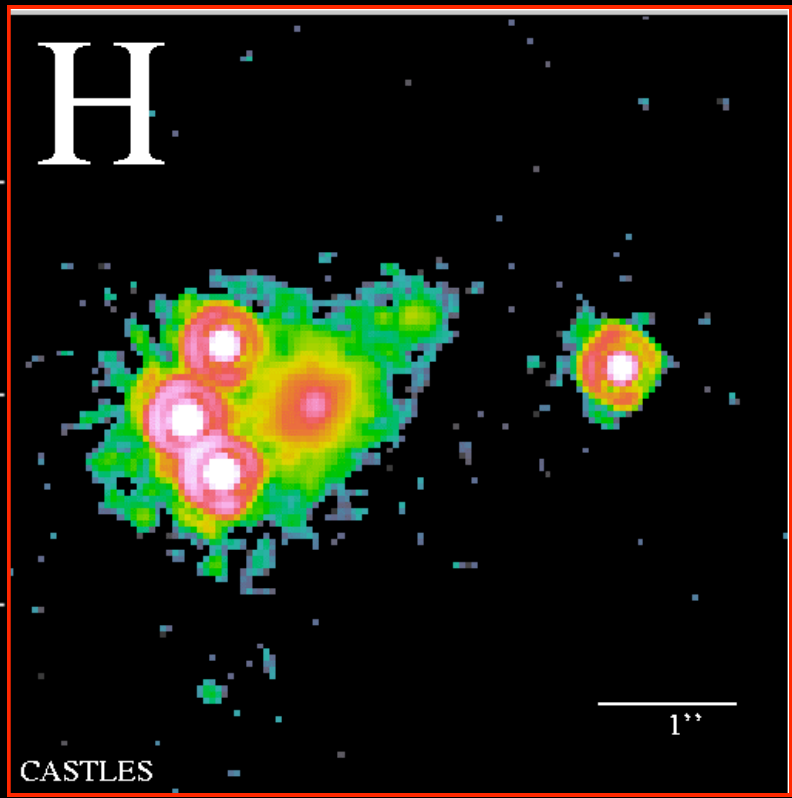

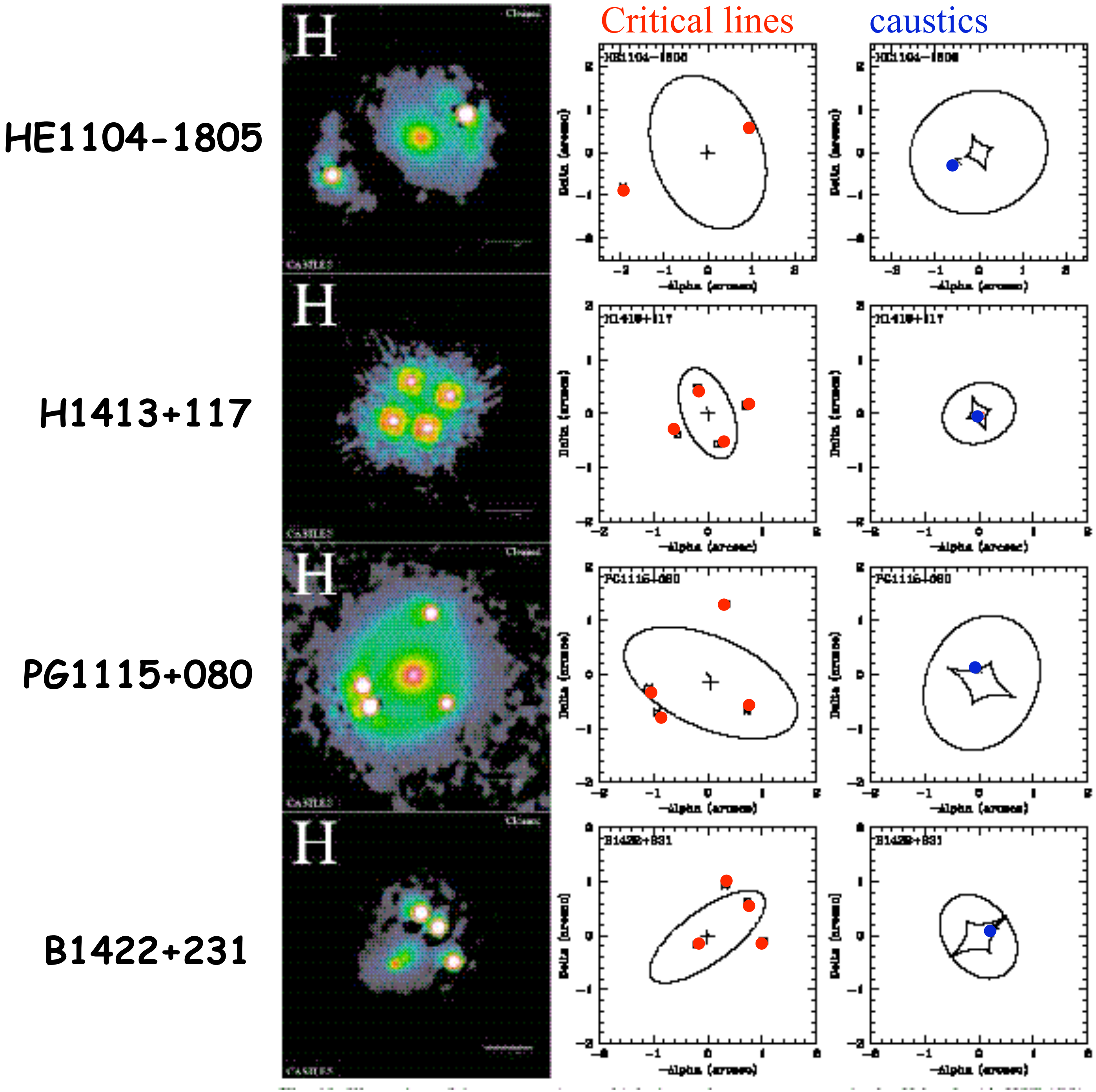

HE1104-1805
H1413+117
PG1115+080
B1422+231
Critical lines
caustics
H
HE1104-1805
H1413+117
PG1115+080
B1422+231
-Alpha (arcsec)
Delta (arcsec)
CASTLES

Quasar time delays, H_0 and galaxy mass profiles

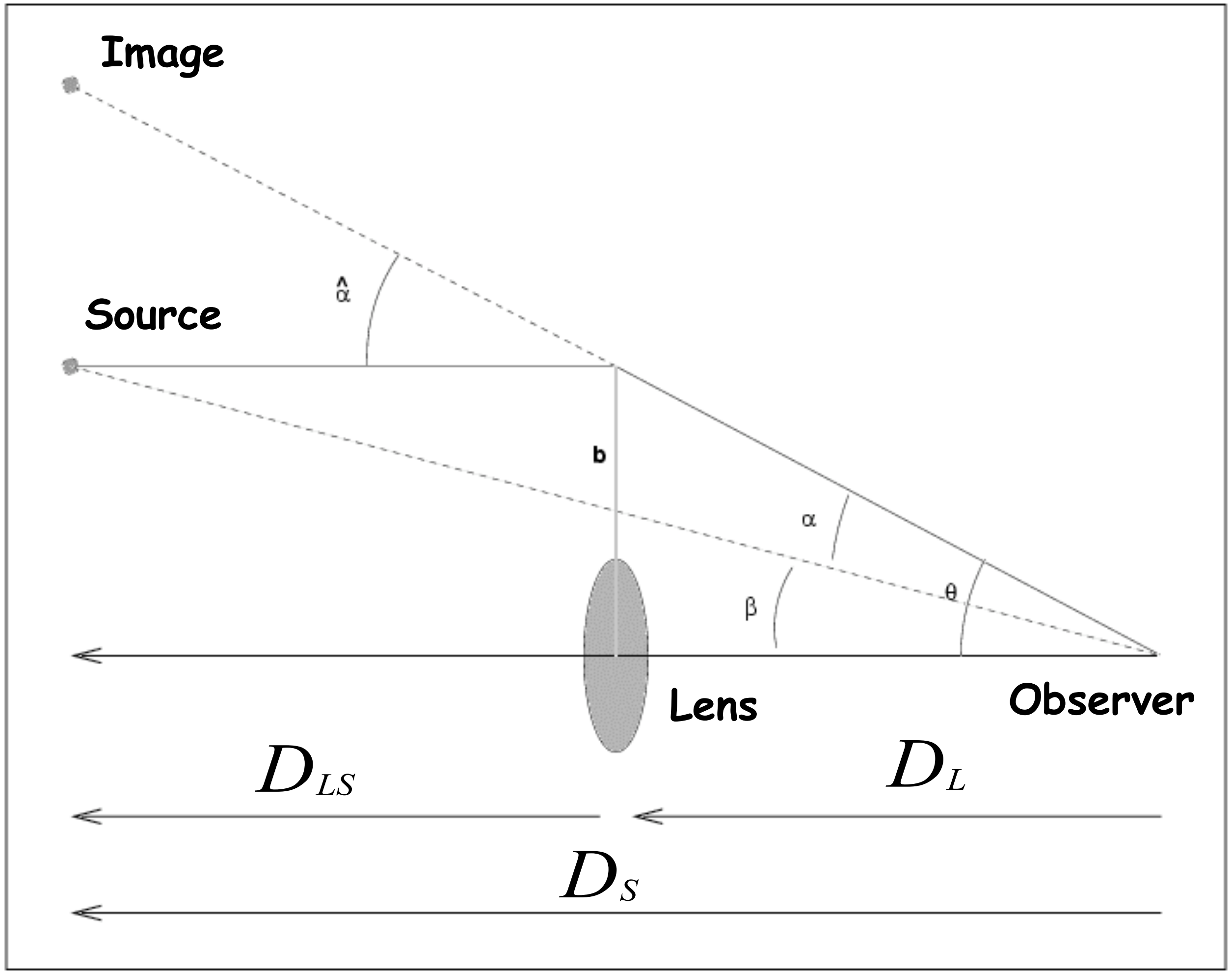

$$t(\vec{\theta}) = \tfrac{1}{2}(1+z_{\rm L})\frac{D_{\rm L}D_{\rm S}}{cD_{\rm LS}}(\vec{\theta}-\vec{\beta})^2 - (1+z_{\rm L})\frac{8\pi G}{c^3}\nabla^{-2}\Sigma(\vec{\theta}).$$

Geometry (plus Ho) **Mass distribution**

WFI 2033-4723

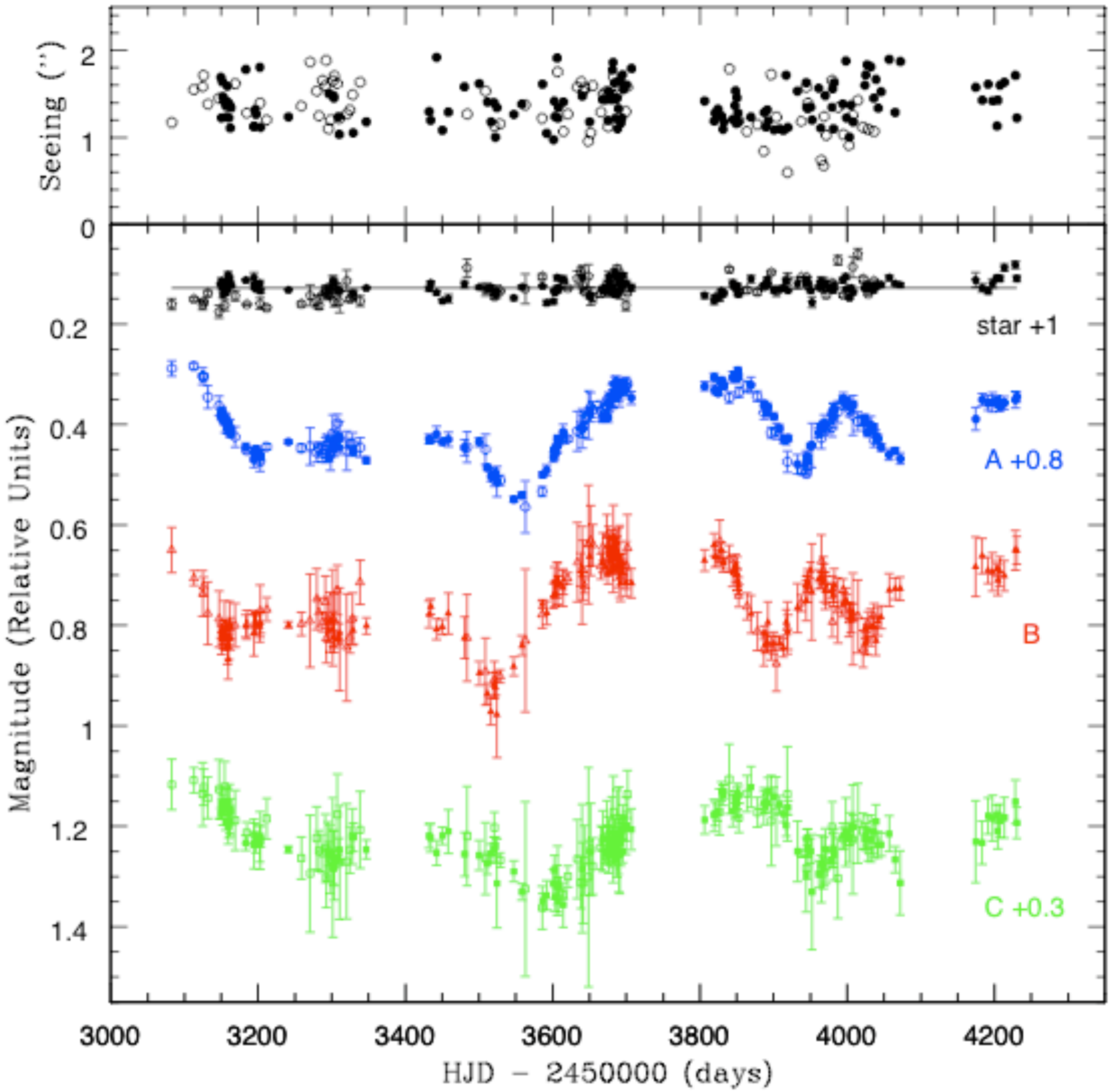

Vuissoz et al. 2008

Quasar microlensing

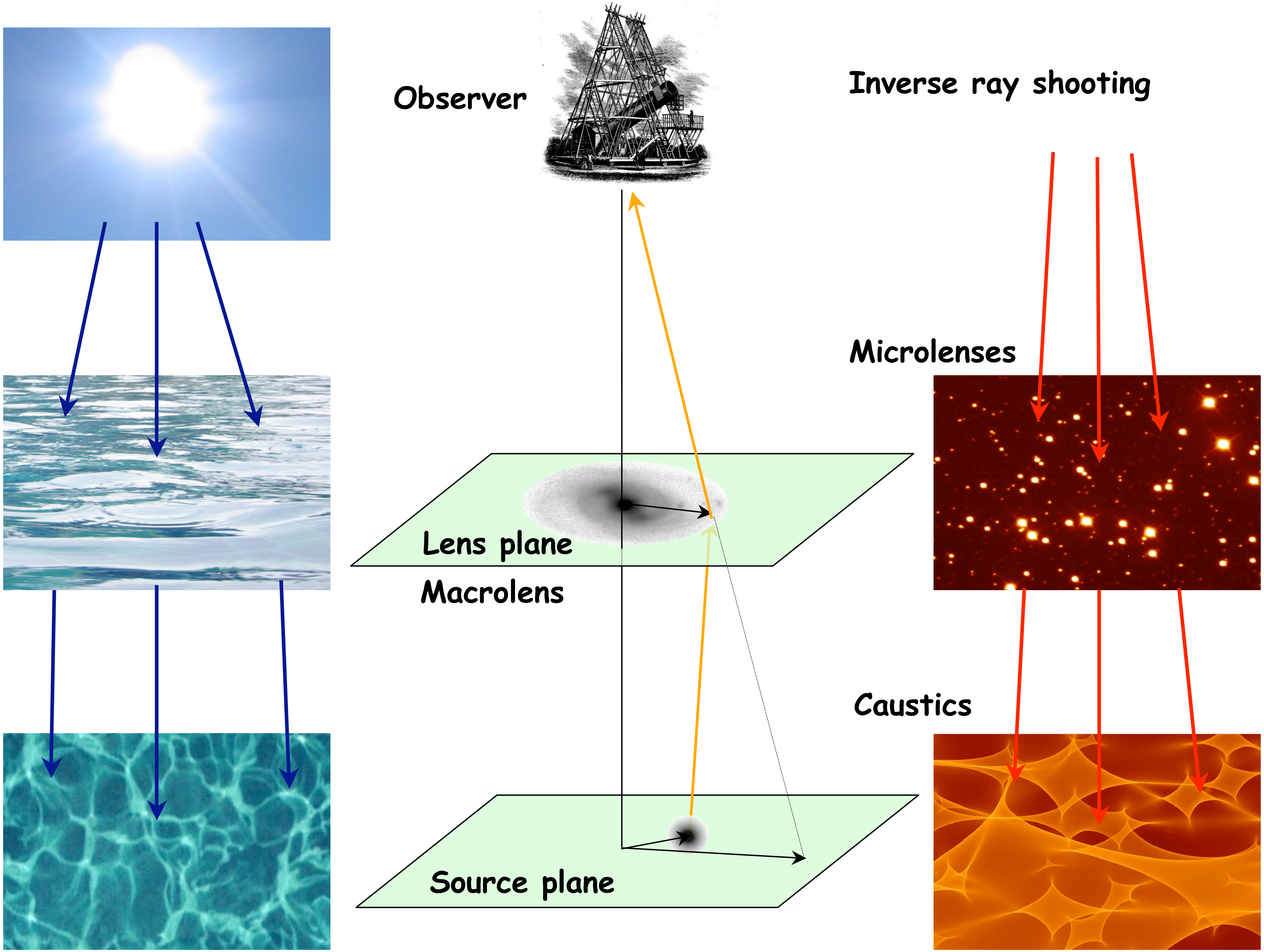
Observer
Inverse ray shooting
Microlenses
Lens plane
Macrolens
Caustics
Source plane

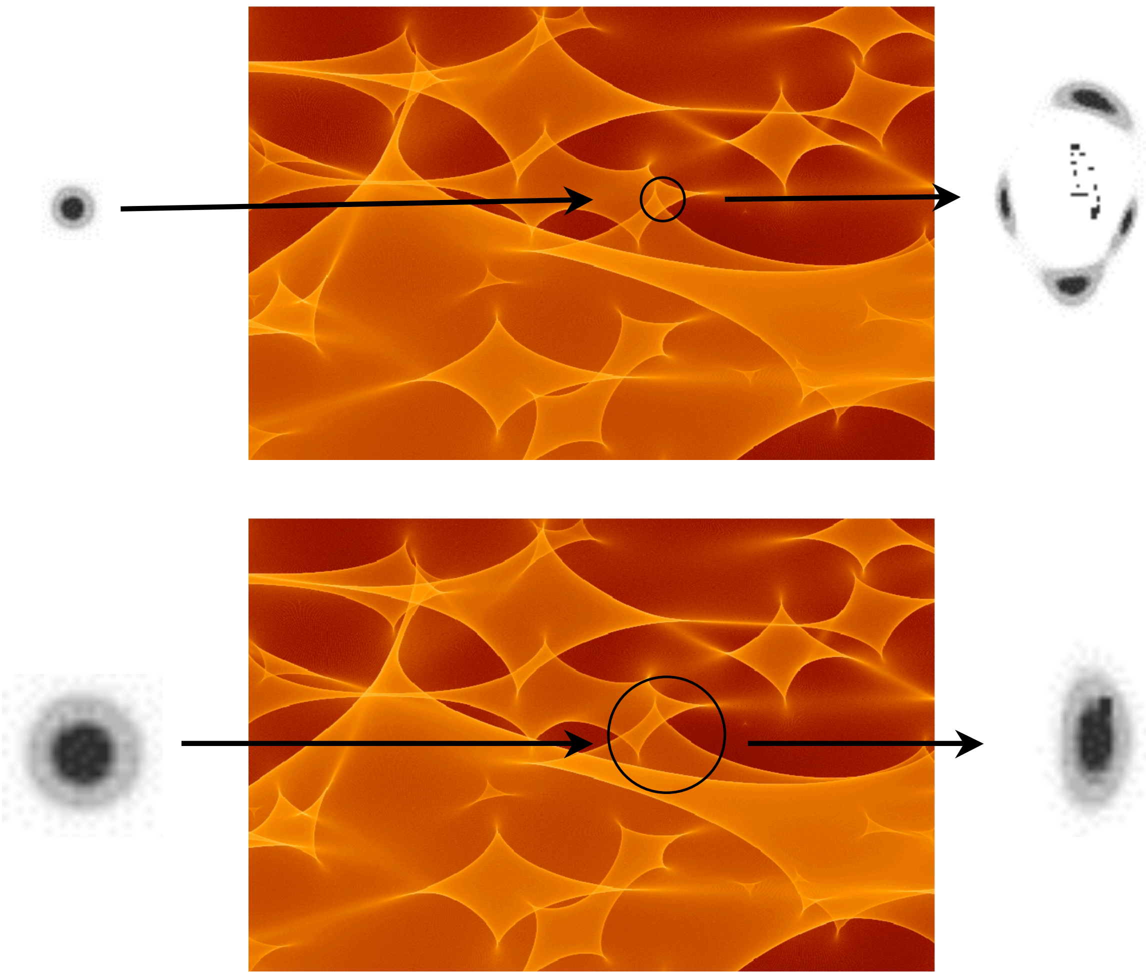

Small sources are fully magnified

Only parts of large sources are magnified

Smaller sources get more magnified

Microlensing light curves of sources with different angular sizes can be easily predicted and compared with observations. So far only very little information has been gathered on <u>chromatic</u> microlensing variations

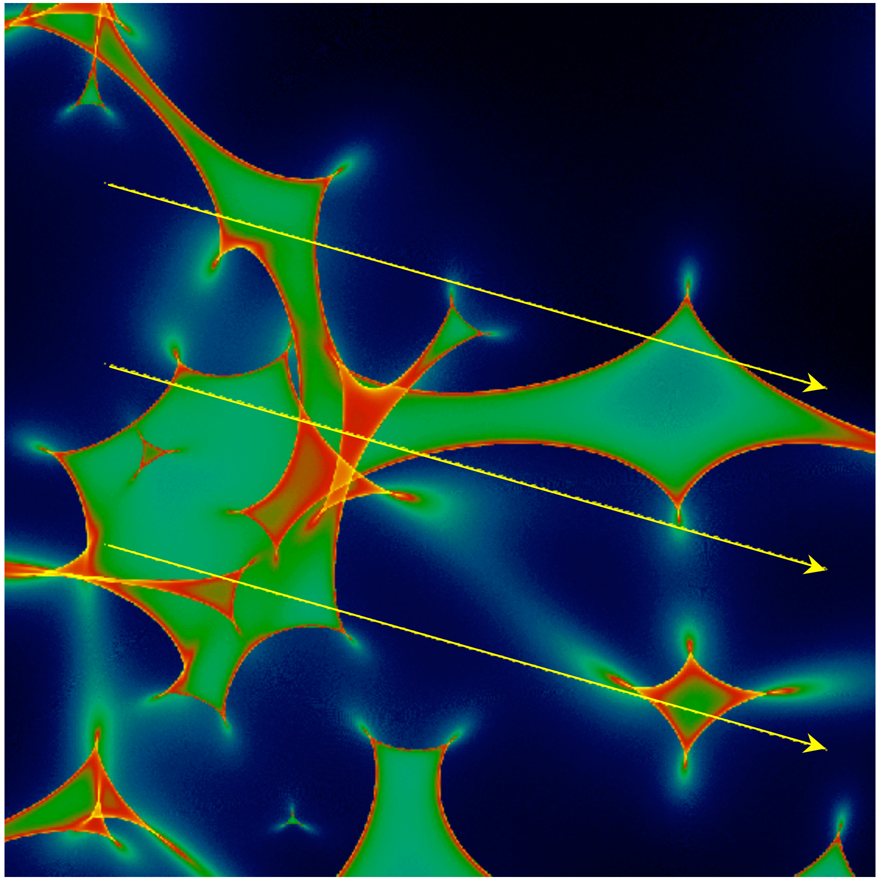

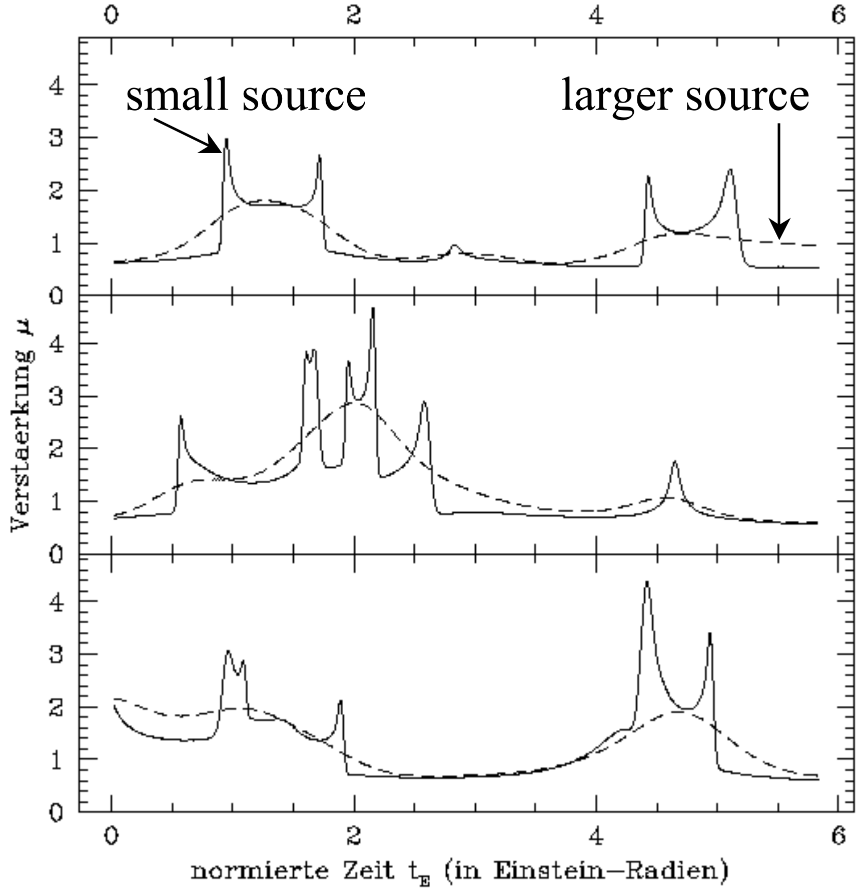

Courtesy J. Wambsganss

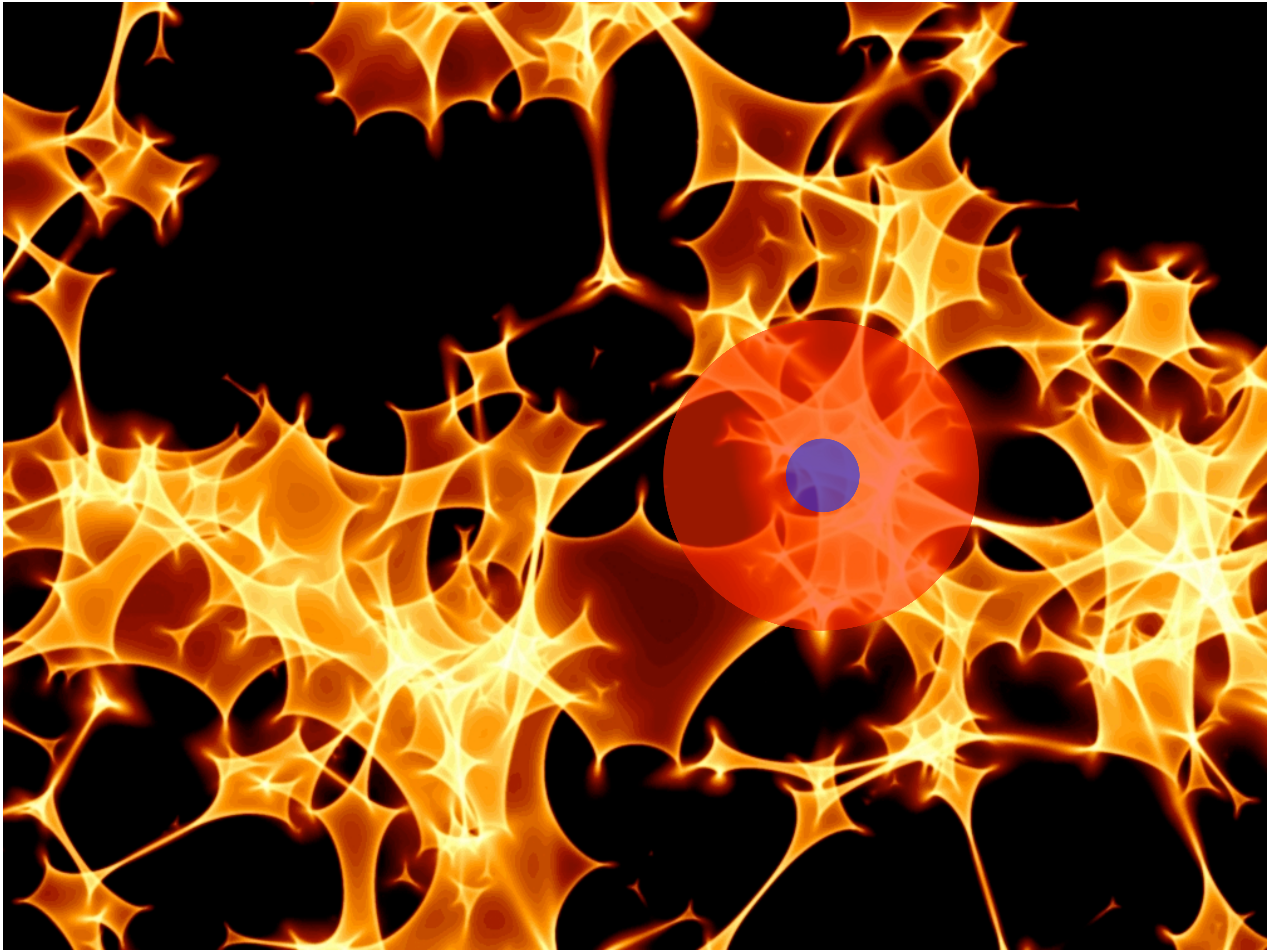

Motivation

Use chromatic microlensing to constraint the energy profile of quasar accretions disks

<u>Requires:</u>

- clear microlensing events
- remove the time delay effect
- good sampling over several years
- broad wavelength coverage
- deblend the quasar images and the lensing galaxy
- accurate flux calibration over the whole monitoring

Spectrophotometric monitoring of the Einstein Cross

Discovery of the Einstein Cross:
a first lucky case

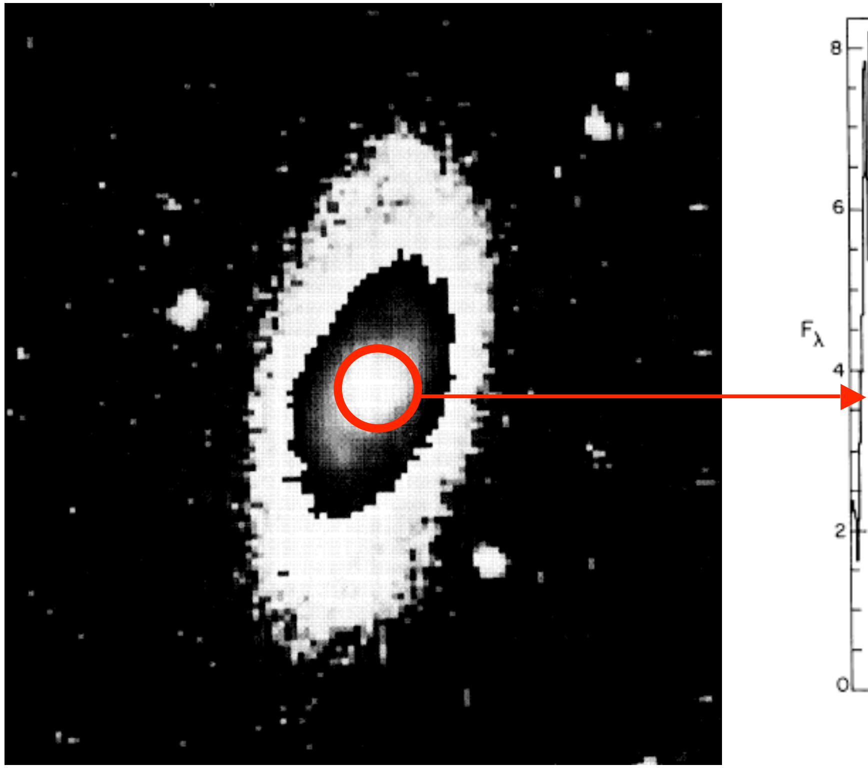

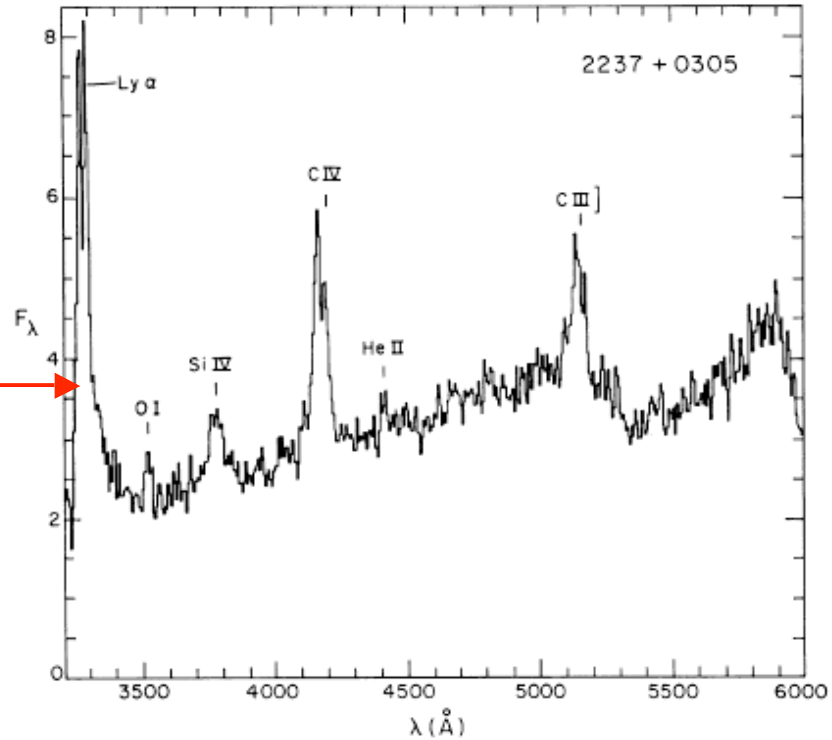

Huchra et al. 1985, AJ 90, 691

Discovery of the Einstein Cross:
a first lucky case

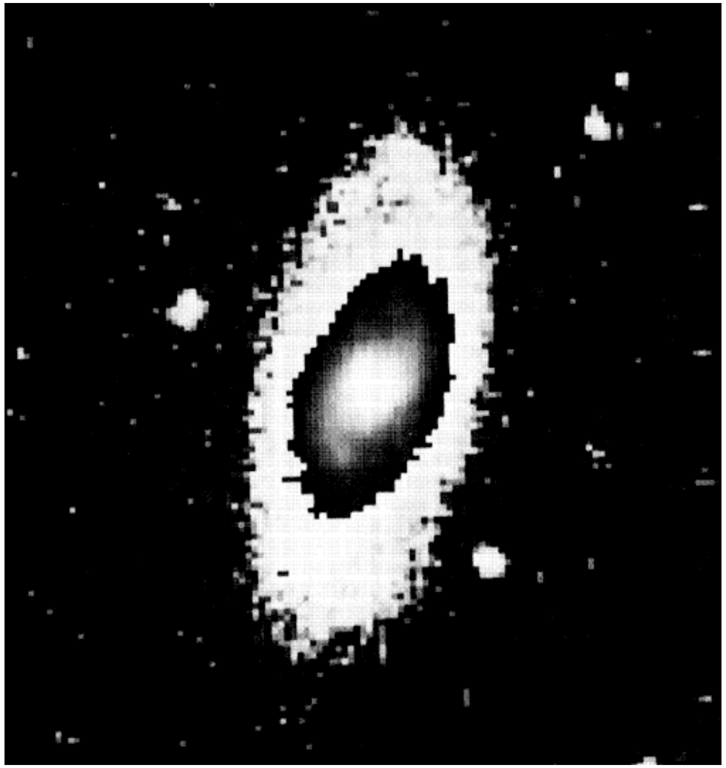

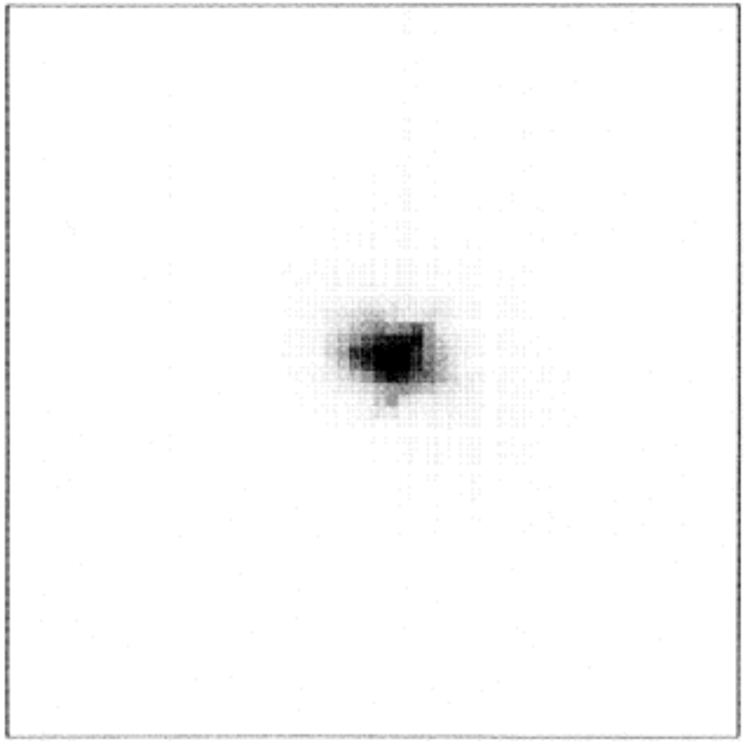

Schneider et al. 1988, AJ 95, 1619

Q2237+080 is ideal for microlensing studies

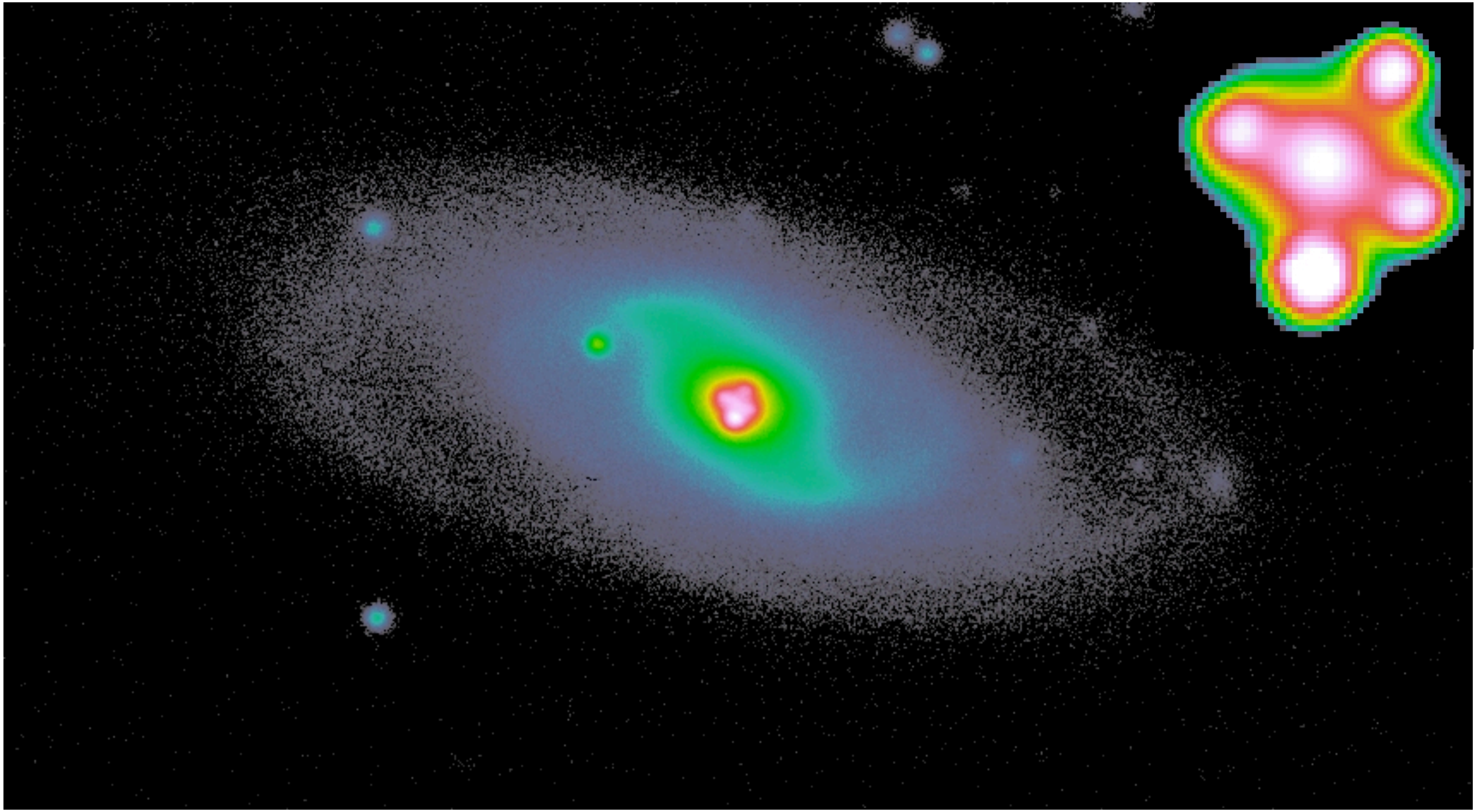

VLT/FORS1 « snapshot » of the Einstein Cross in the R-band

OGLE V-band light curves from 1998 to 2008

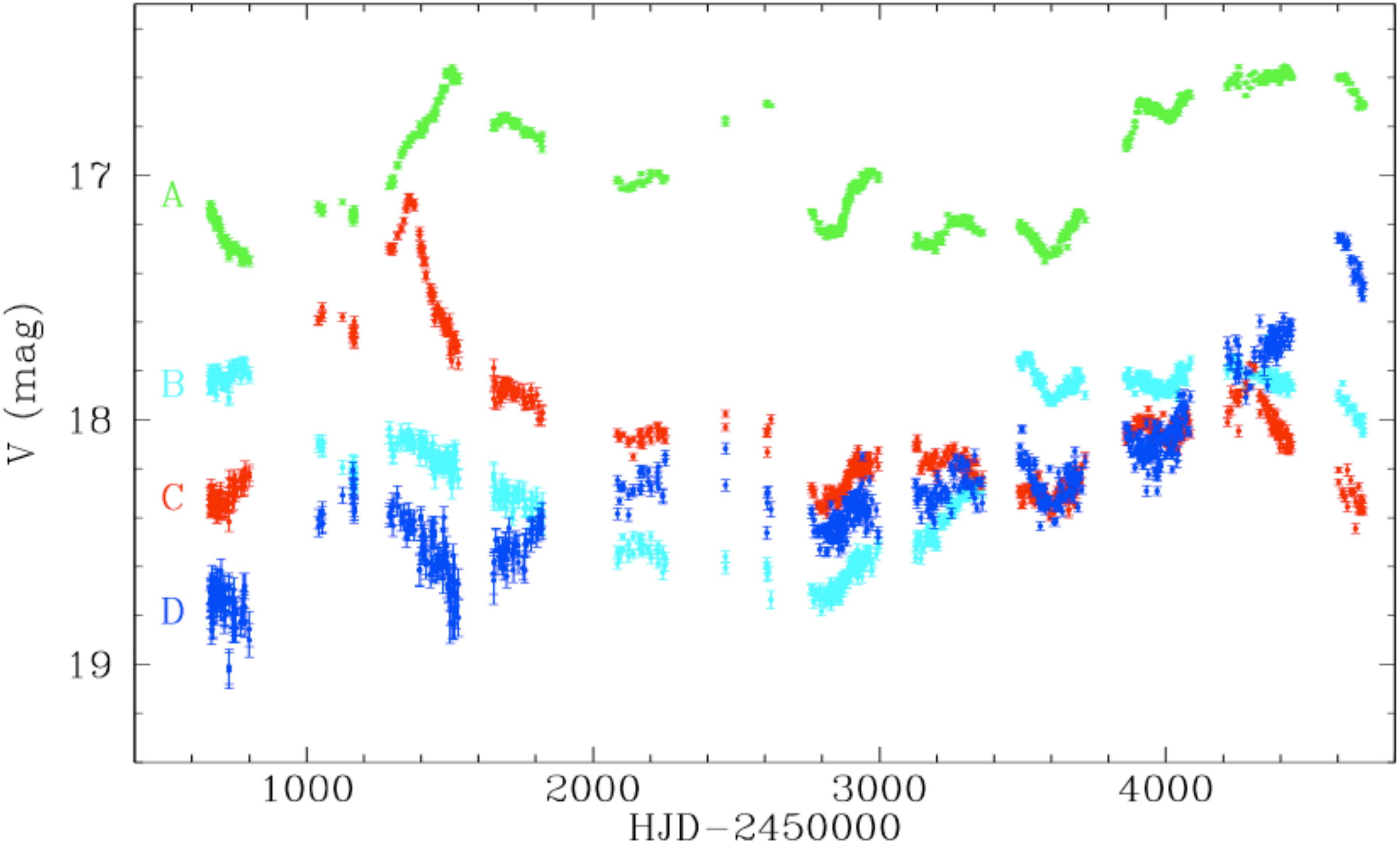

(Wozniak et al. 2000, Uldalski et al. 2008 + recent update)

OGLE V-band light curves from 1998 to 2008

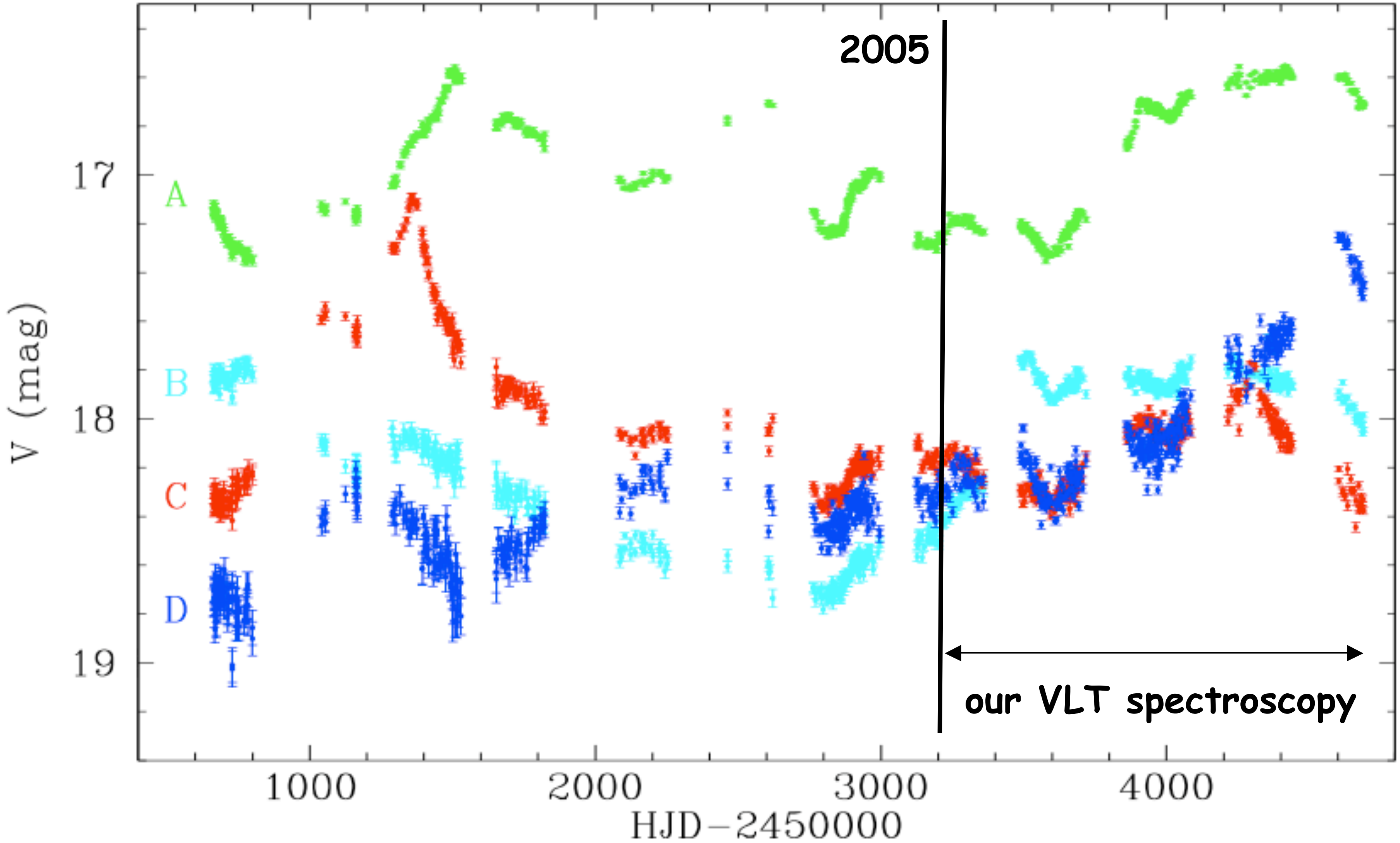

(Wozniak et al. 2000, Uldalski et al. 2008 + recent update)

Spectrophotometric monitoring of the Einstein Cross

- Large Program at the VLT
- 60 hours with FORS1/VLT in total
- Optical spectra of all 4 components for 42 epochs
- Use of the atmospheric refraction corrector

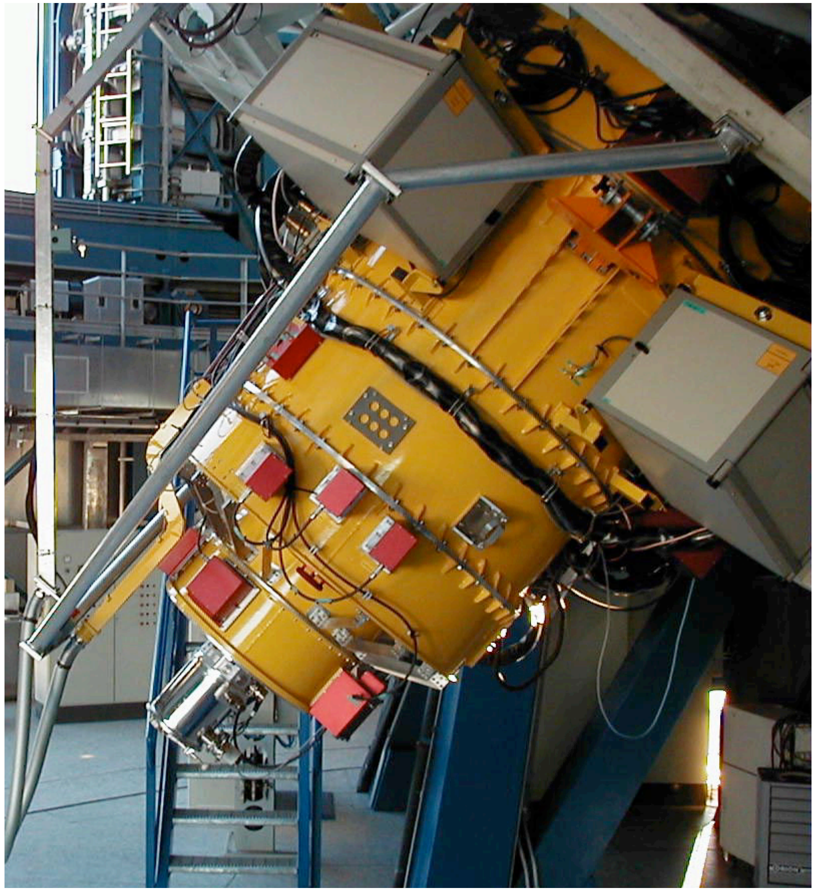

FOcal Reducer and low dispersion Spectrograph (FORS1)

Extracting the quasar spectra

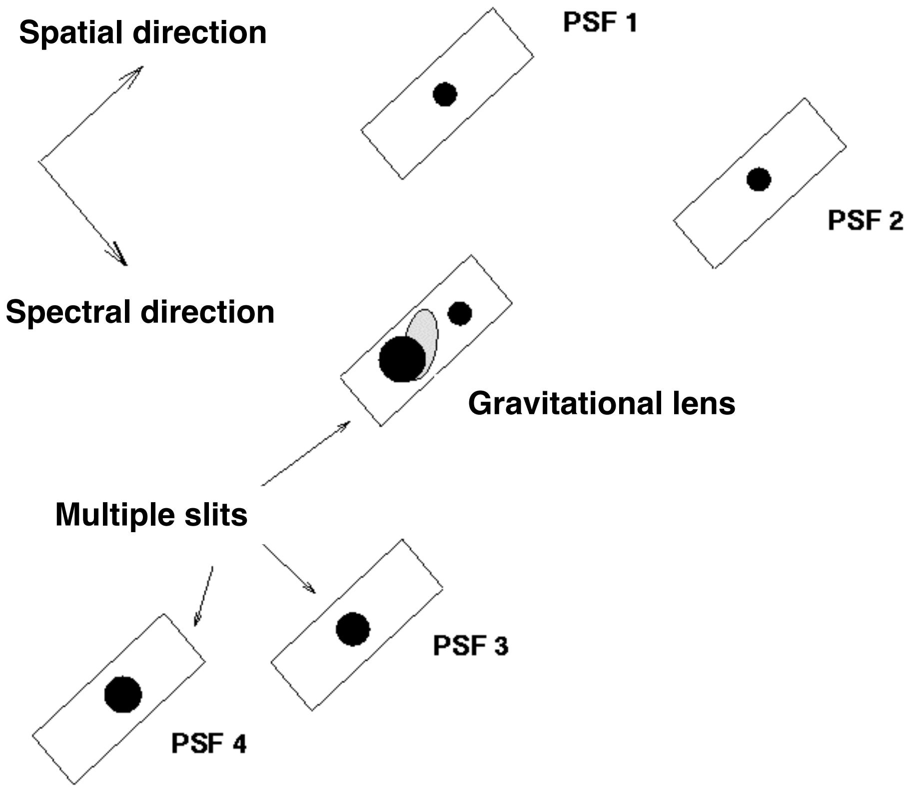

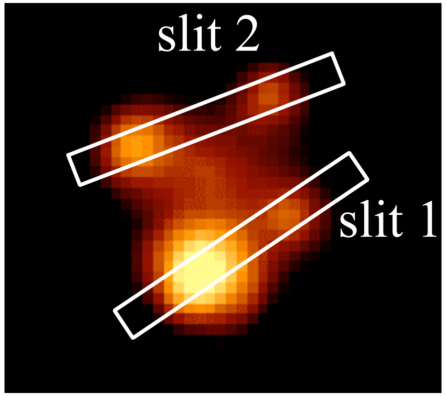

Two masks per epoch

15 days between 2 epochs

4000-8000 Å

0.7" slit

R~400 (2.7 Å per pixel)

Seeing < 0.8 arcsec

Exp. Time: 1620 s

42 epochs in total

Courbin et al. 2000, ApJ 1136, 529

Extracting the quasar spectra

Example of a spectrum taken in mask1 (comps. A+D)

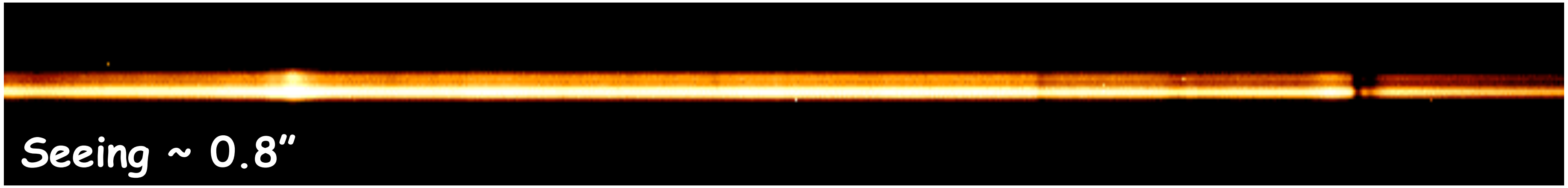

↓ Spatial deconvolution

Components A+D alone

+

Lensing galaxy alone

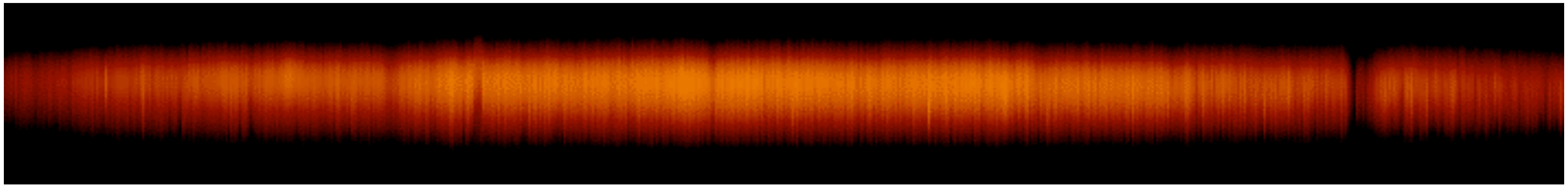

Extracting the quasar spectra

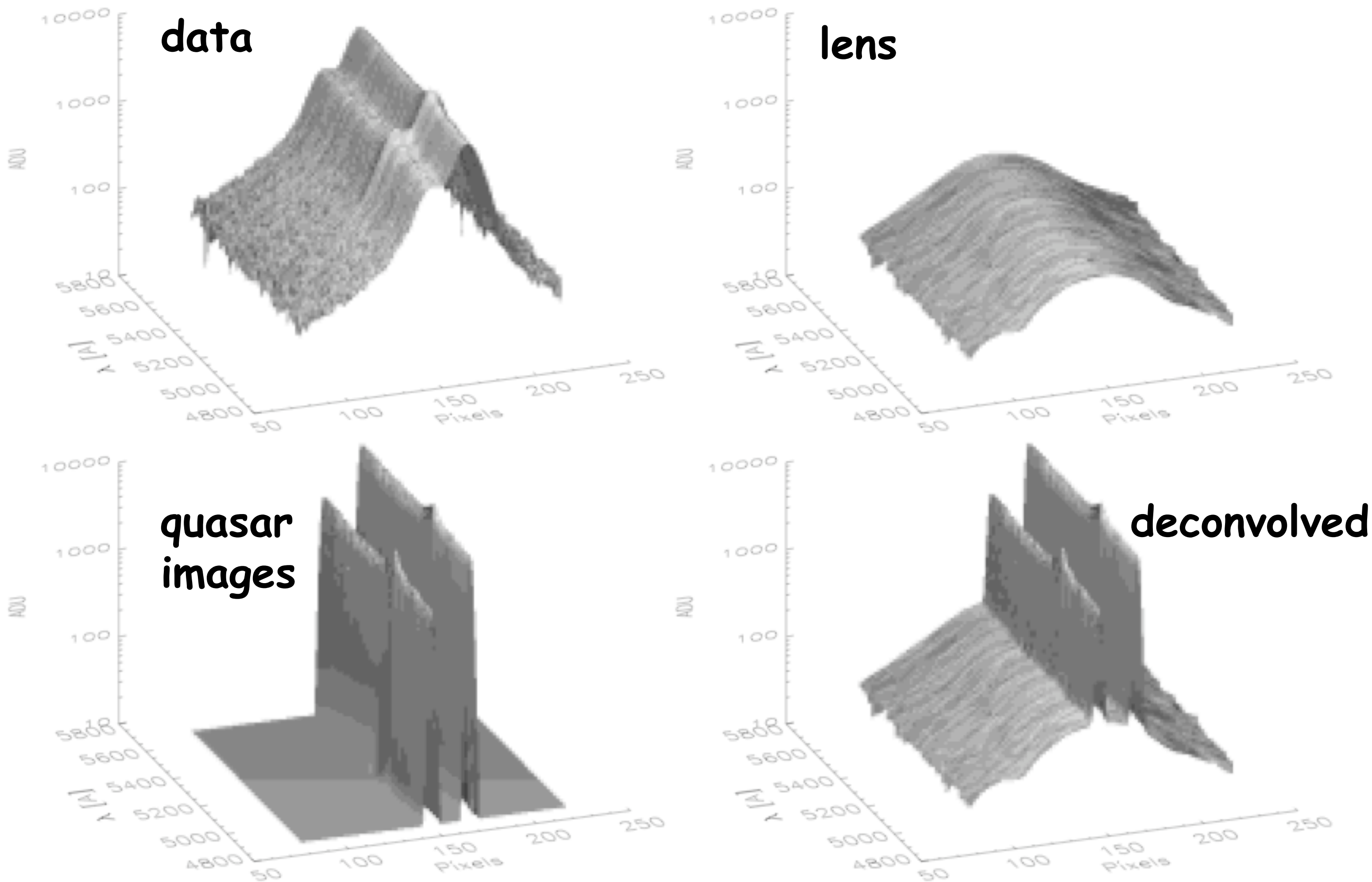

Flux cross-calibration between epochs

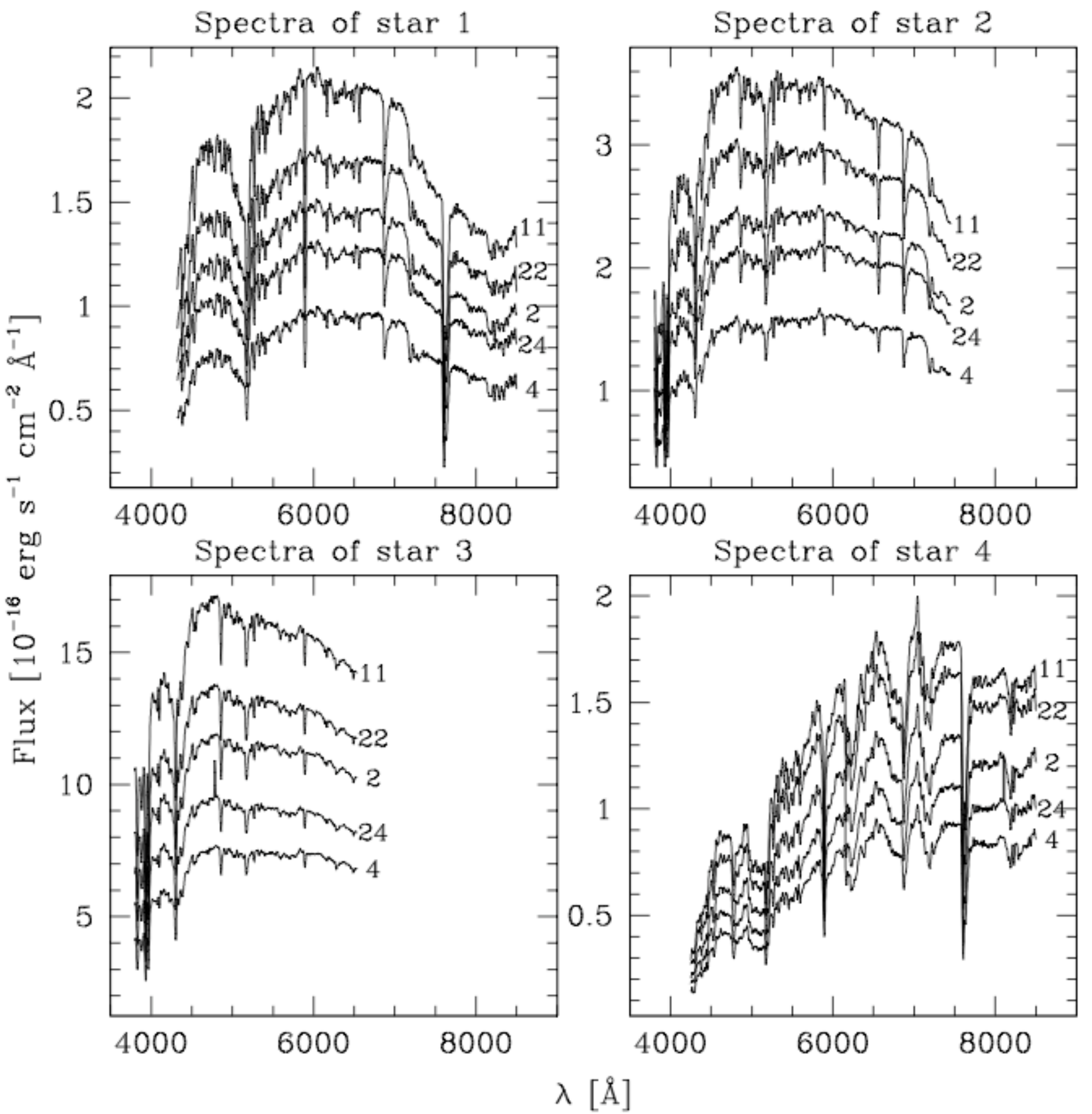

Flux cross-calibration between epochs

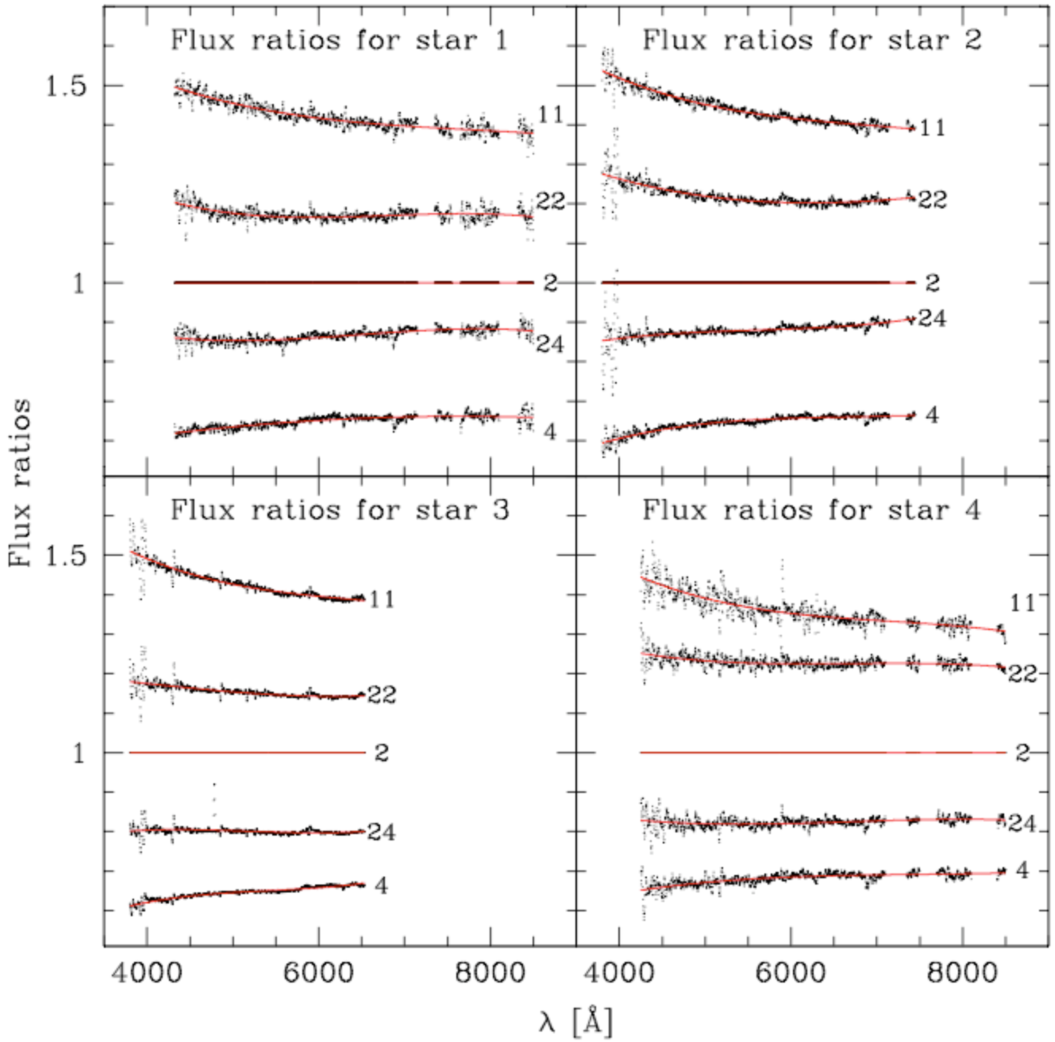

In addition FORS1 on the VLT has an atmospheric refraction corrector

Sanity check using the OGLE photometry

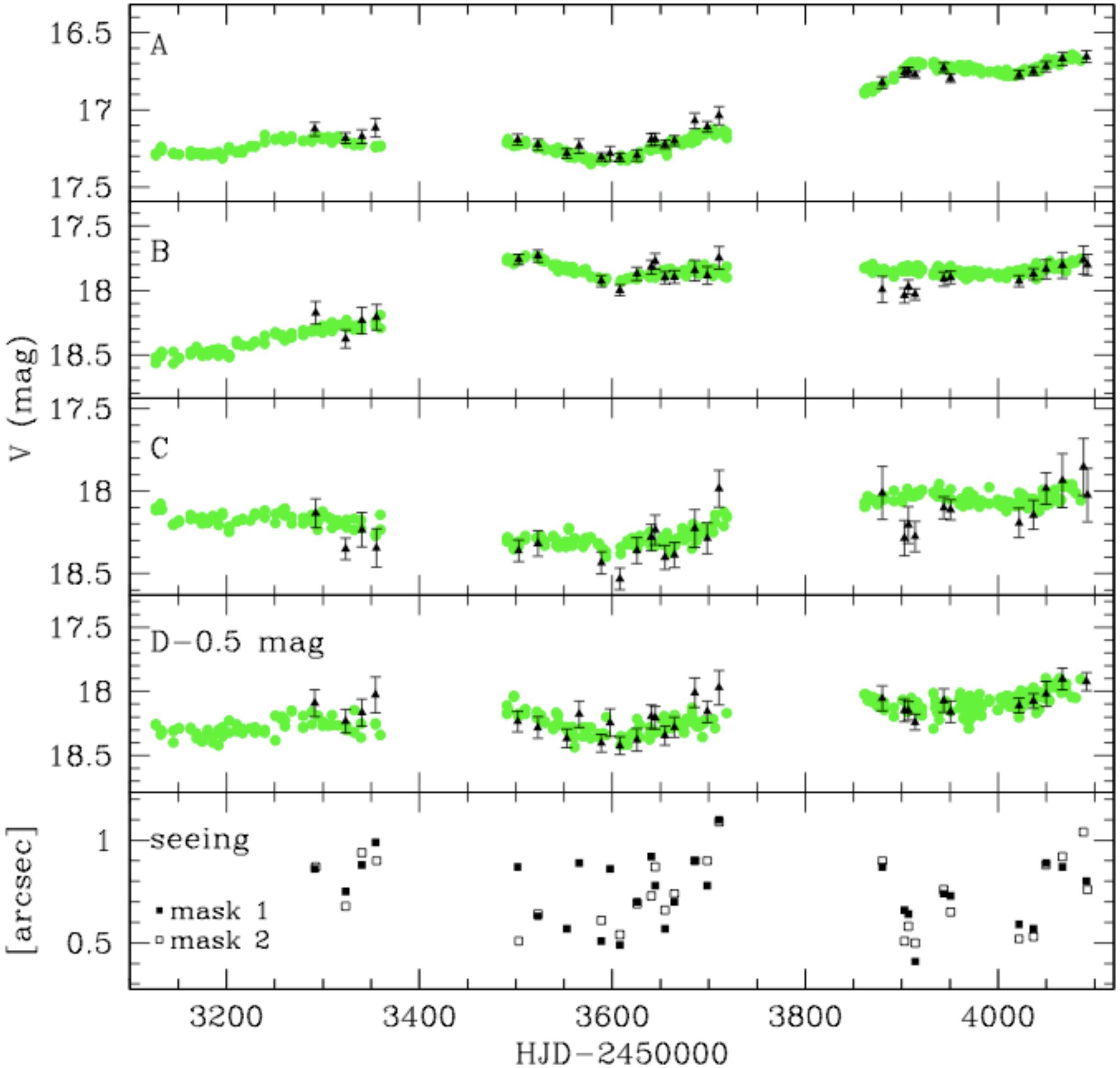

+ the spectra of the lens galaxy in the two masks are identical

Last step: decomposition of the 1D spectra

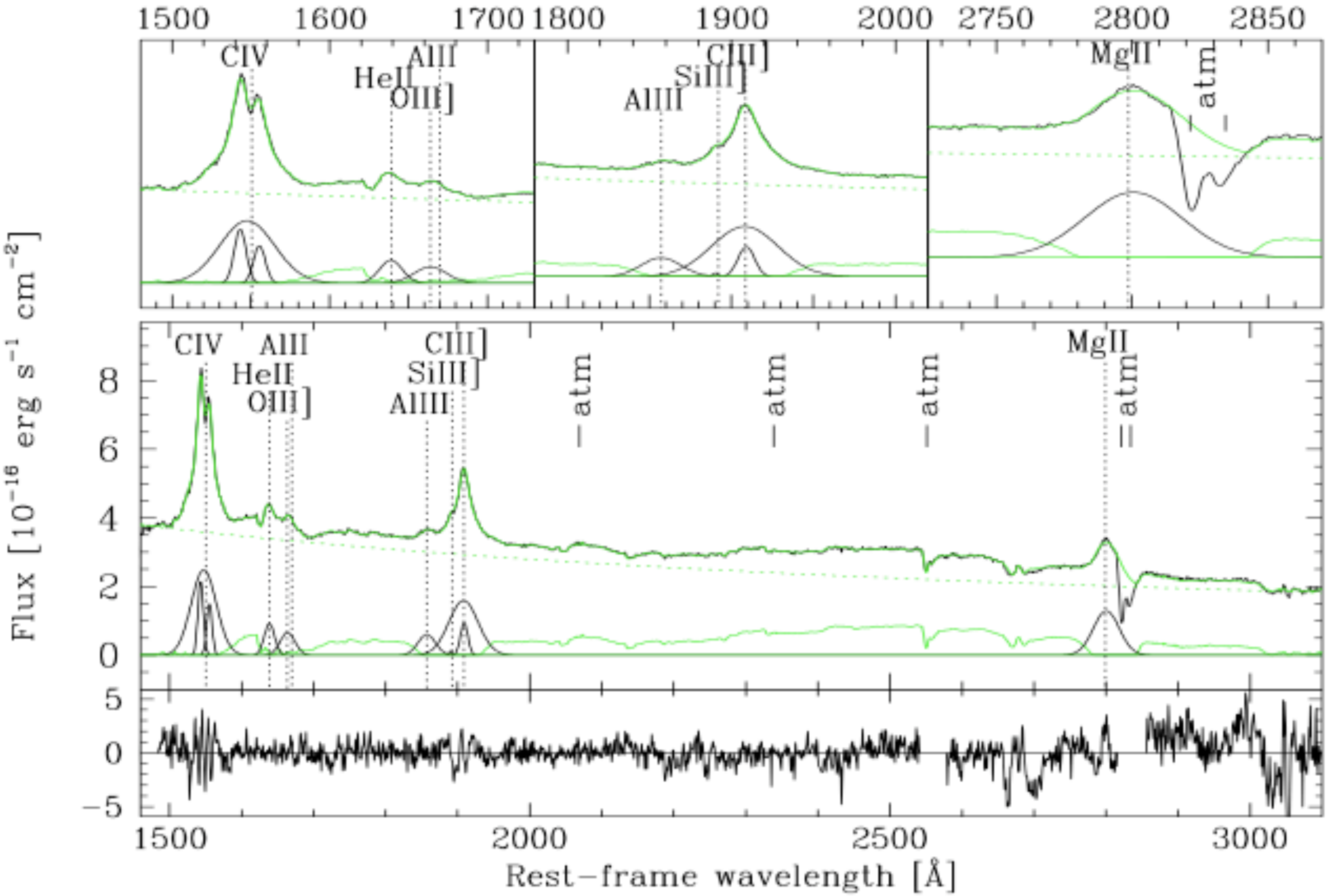

Sum of Gaussian emission lines + power law continuum
+ template for the iron optical emission (from Vestergaard 2001)

Einstein Cross:

Image A

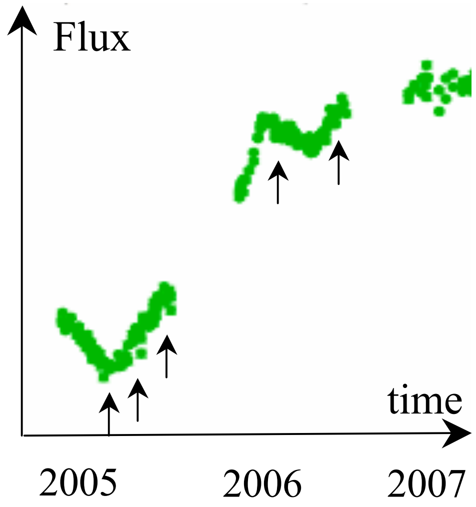

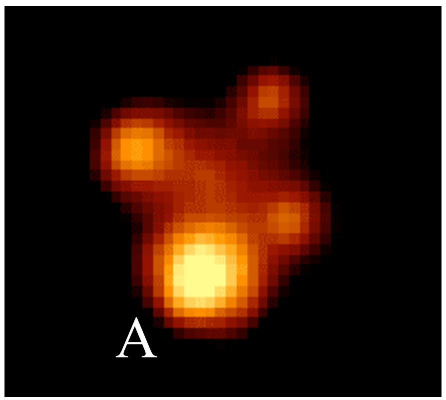

VLT FORS1 R-band

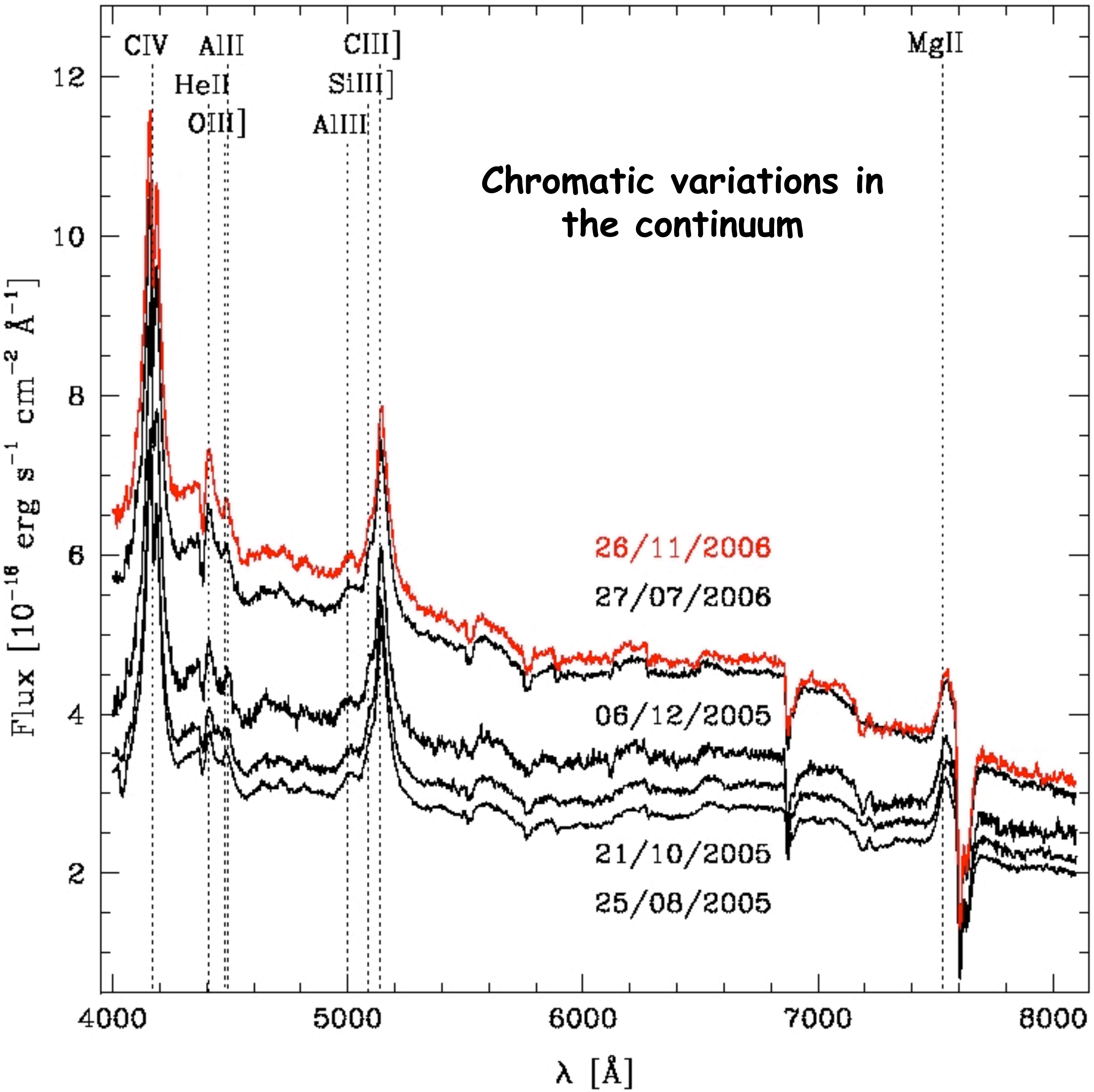

Einstein Cross:

Image A

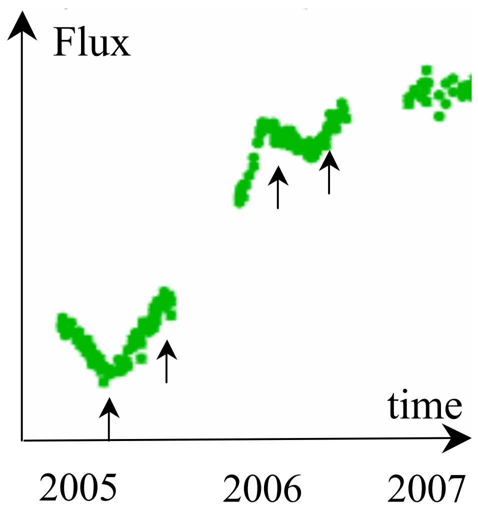

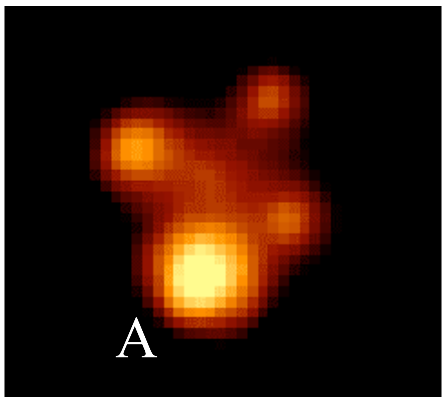

Intensity and profile variations of the BELs

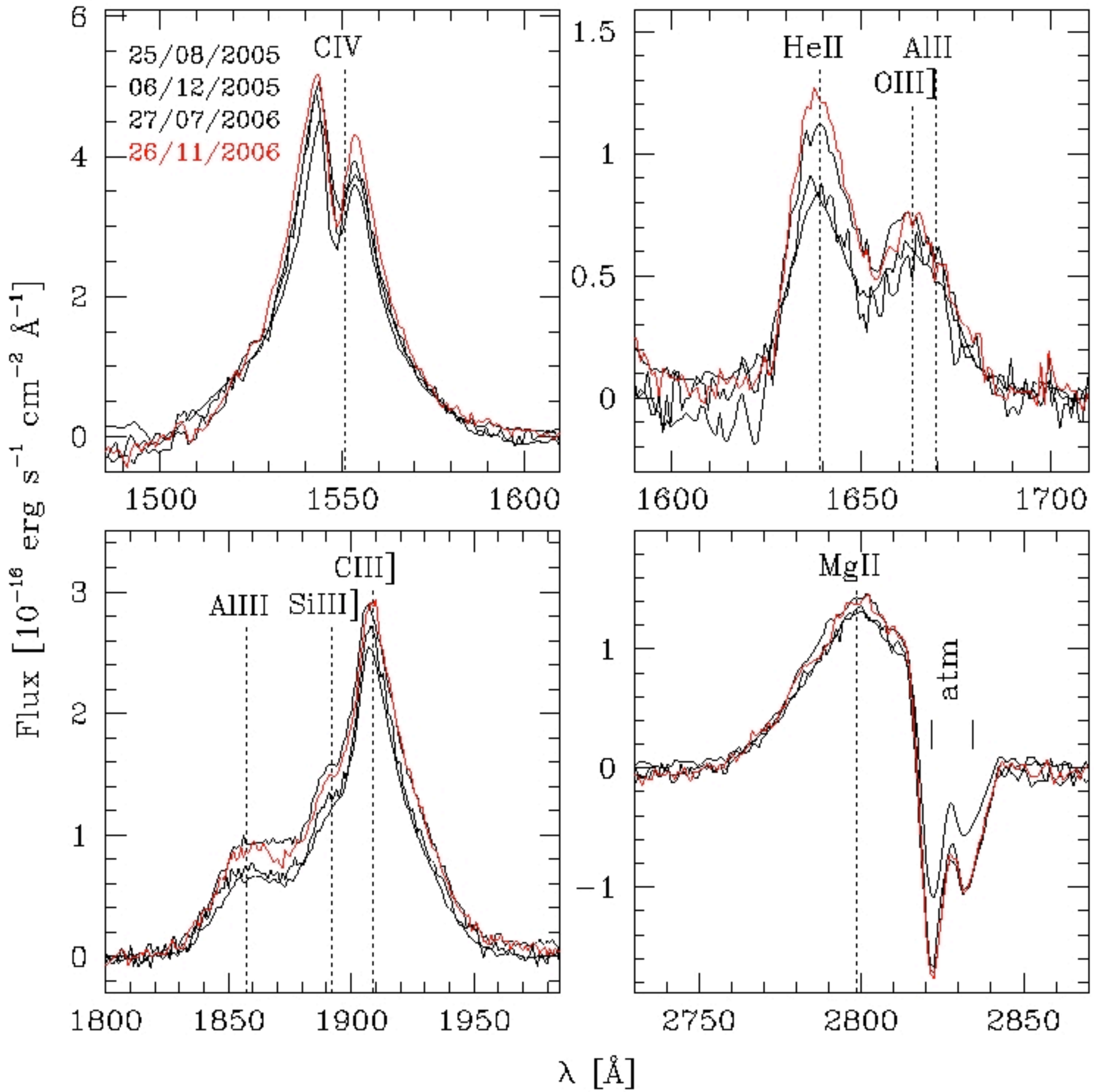

Microlensing simulations

<u>Goal:</u> to measure the energy profile of the accretion disk

$$R \propto \lambda^{\eta}$$

Theory tells us that

η = 1.30 (Shakura & Sunyev, 1973)
η = 1.15 (Agol & Krolik, 2000)
η = 1.75 (Gaskell 2008)

Need to measure source size as a function of distance to the black hole: use microlensing magnification

$$\frac{R}{R_{\mathrm{ref}}} = \left(\frac{\lambda}{\lambda_{\mathrm{ref}}} \right)^{\eta}$$

Microlensing simulations

- Convergence and shear from Kochanek (2004)
- <M> = 0.1 $M_\odot$ (results not sensitive to the mass function)
- Microlensing patterns with 10000 x 10000 pixels: 100 R_E
- 10^{11} ray shootings
- We fit <u>difference light curves</u> in six bands (continuum only)

  1- remove the intrinsic variations

  2- not sensitive to differential extinction

Microlensing simulations

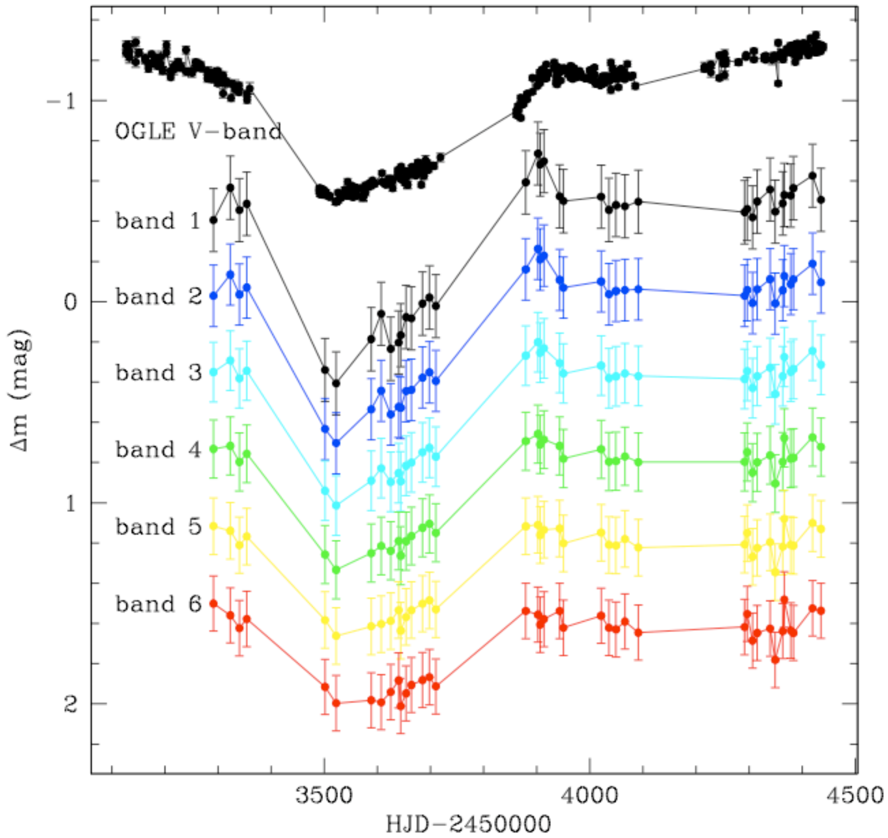

Multiband (200Å) light curves for the continuum (A-B)

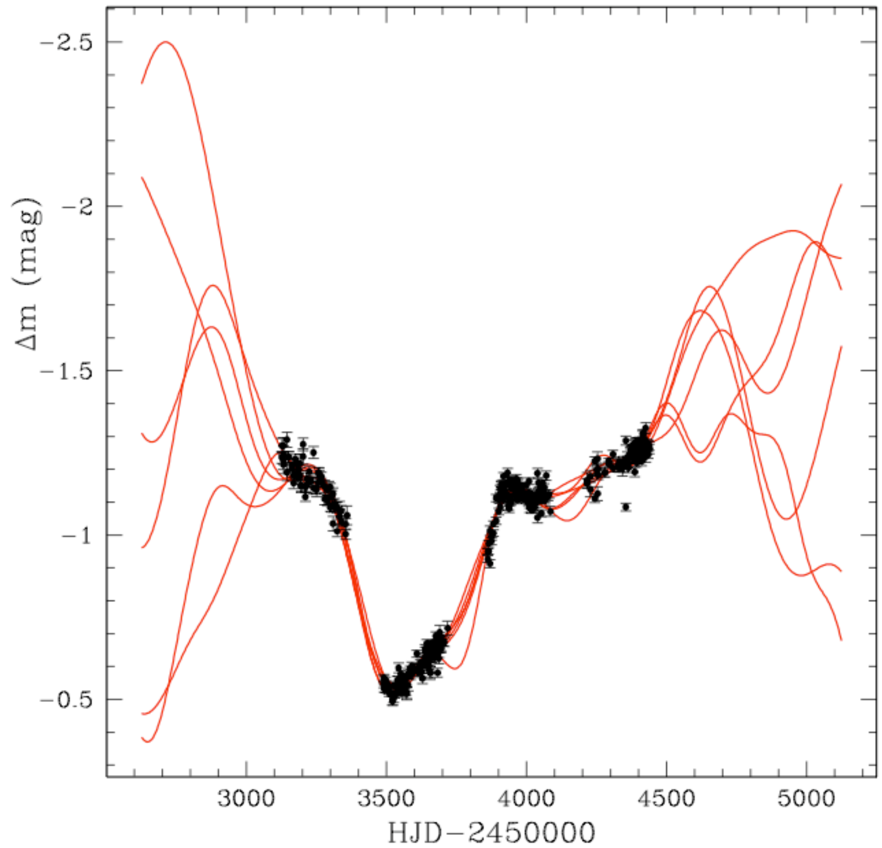

Fit to the V-band OGLE difference light curve (A-B)

Microlensing simulations

- Source shape is Gaussian (but unimportant)
- Choose 45 different source sizes:

$$0.01\ R_E < R < 4\ R_E$$

- For the 45 sizes, sample the source plane with 10000 light curves that fit well the OGLE data
- Library of 45000 "good" trajectories to carry out Bayesian analysis similar to Kochanek (2004) and Anguita et al. (2008)
- Find the best source size for each wavelength, i.e., peak of the probability distribution in radii

Microlensing simulations

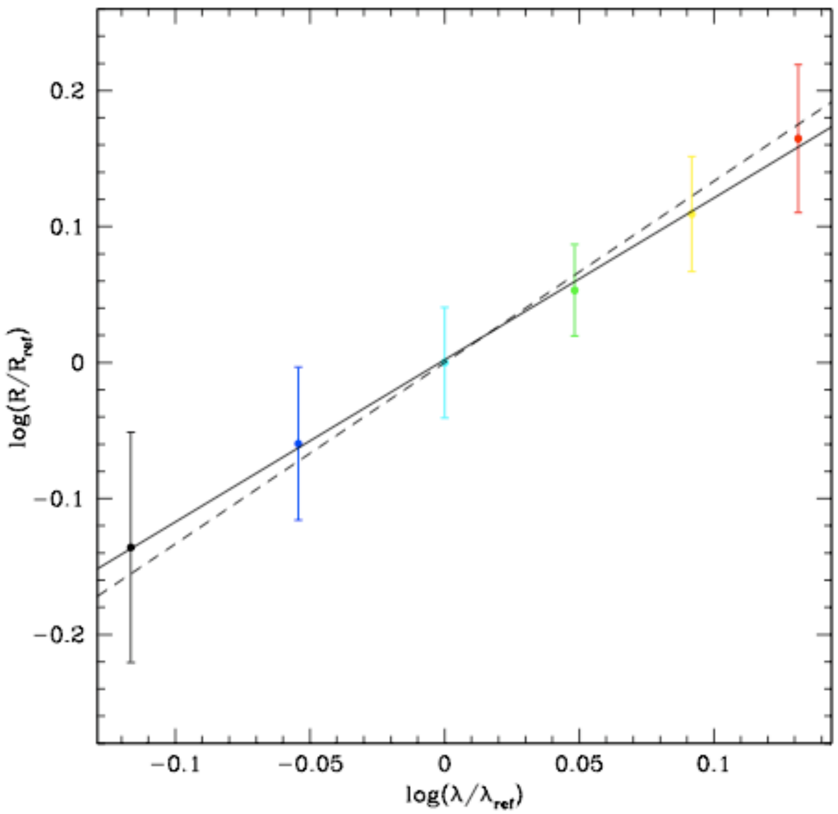

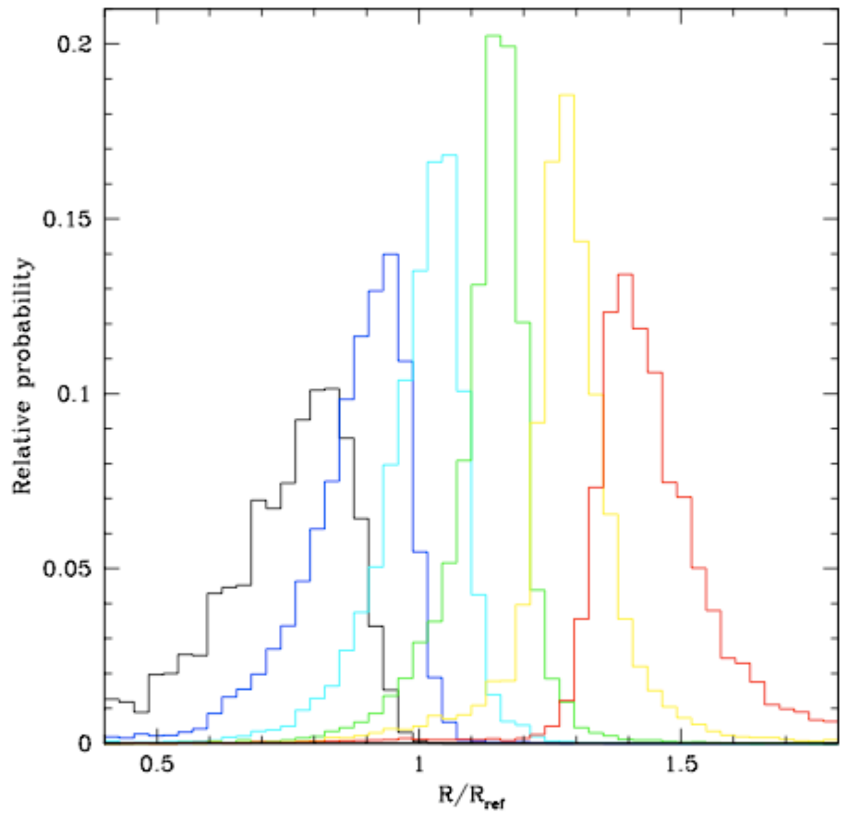

Linear regression to the data gives η=1.2±0.3

Main results

- 42-epochs VLT spectra of the 4 individual quasar images
- Observations from Oct. 2004 to Dec. 2007
- S/N~100 over 4000-8000 Å
- Energy profile is proportional to $\lambda^{1.2\pm0.3}$
- Best compatible with prediction from Agol and Krolik (2000), (slope η=1.14, accretion disk powered by black hole spin)
- We do not rule out Shakura-Sunyaev (slope η=1.3) yet.
- The Broad Emission Line also vary, both in intensity and profile
- High ionisation lines vary more than low ionisation lines, in agreement with reverberation mapping studies

Continuing with the quadruple RX J1131-123

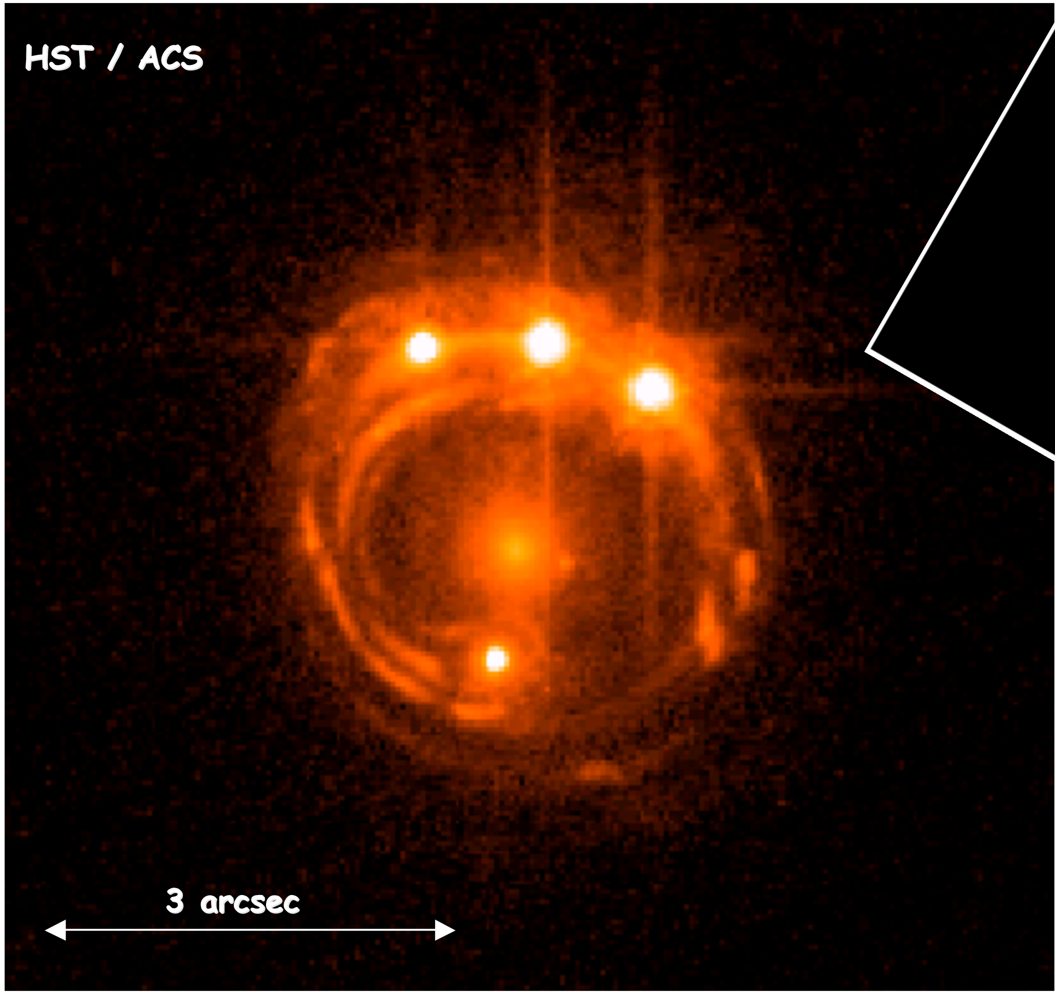

1.2 m Euler (La Silla)

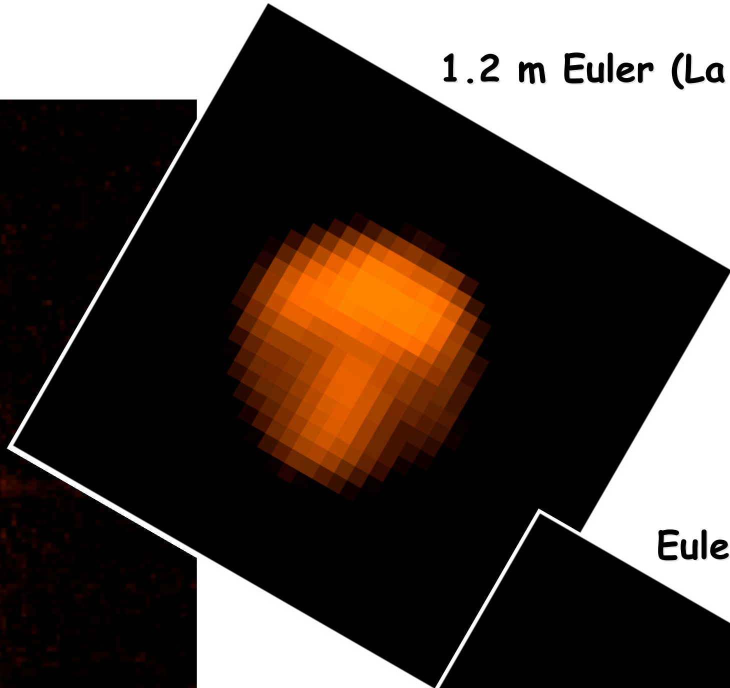

Euler: deconvolved

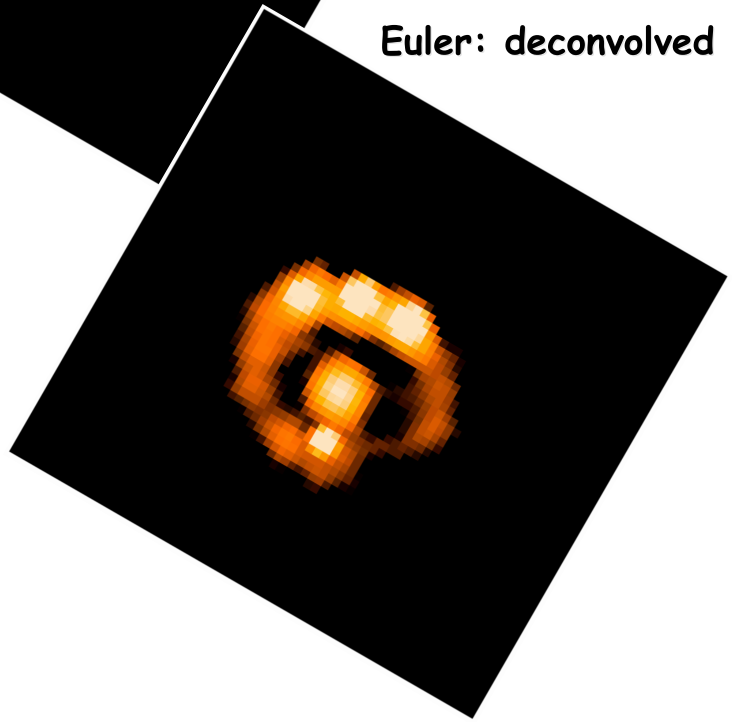

(Sluse et al. 2003, A&A 406, L43,
using data from CASTLE)

Main results

Observational details in Paper I:

Eigenbrod, Courbin, Sluse, Meylan, Agol, 2008, A&A 480, 647

Microlensing simulations in Paper II:

Eigenbrod, Courbin, Meylan, Agol, Anguita, Schmidt, Wambsganss
(in press in A&A, arXiv:0810.0011)

VLT monitoring of RXJ1131-123 has started

PI: Sluse

Questions

Questions

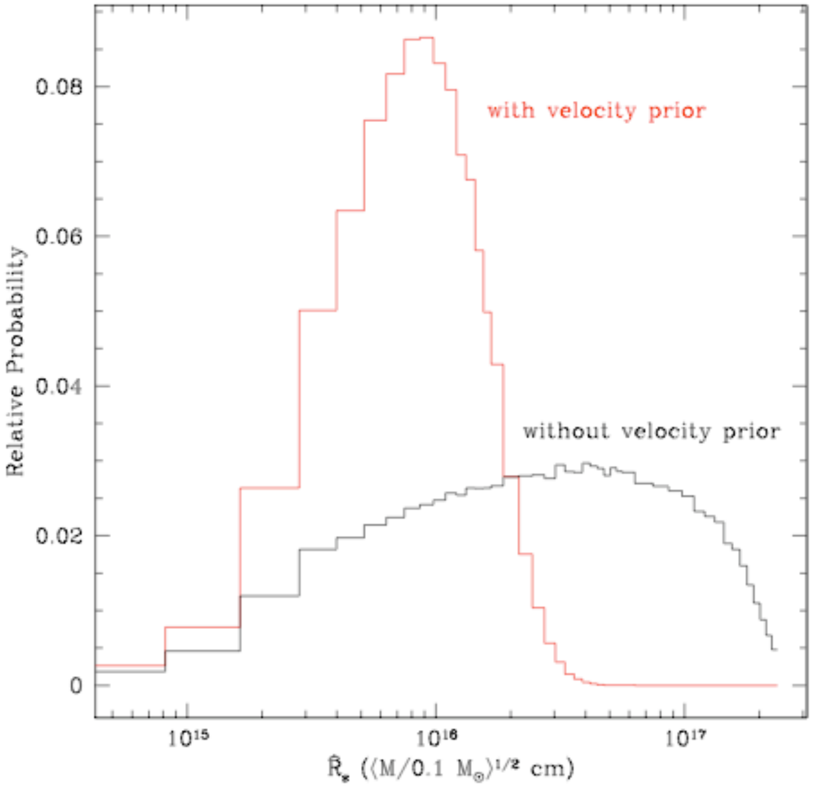

with velocity prior
without velocity prior
Relative Probability
0.08
0.06
0.04
0.02
0
10^{15}
10^{16}
10^{17}
$\hat{R}_*$ ($(M/0.1\ M_\odot)^{1/2}$ cm)

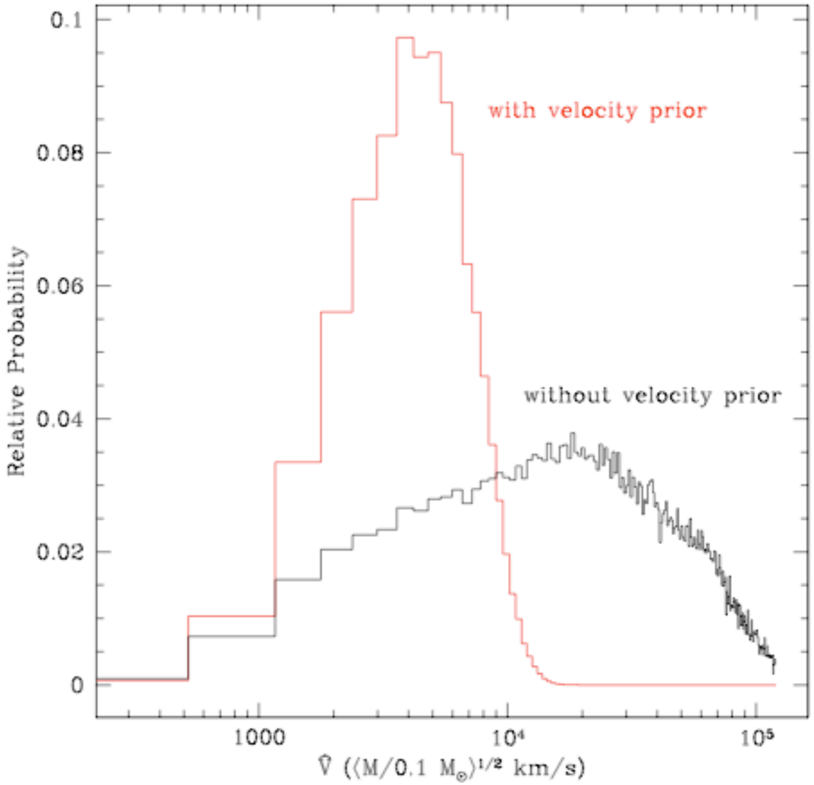

with velocity prior
without velocity prior
Relative Probability
0.1
0.08
0.06
0.04
0.02
0
1000
10^4
10^5
$\hat{V}$ ($(M/0.1\ M_\odot)^{1/2}$ km/s)

Questions

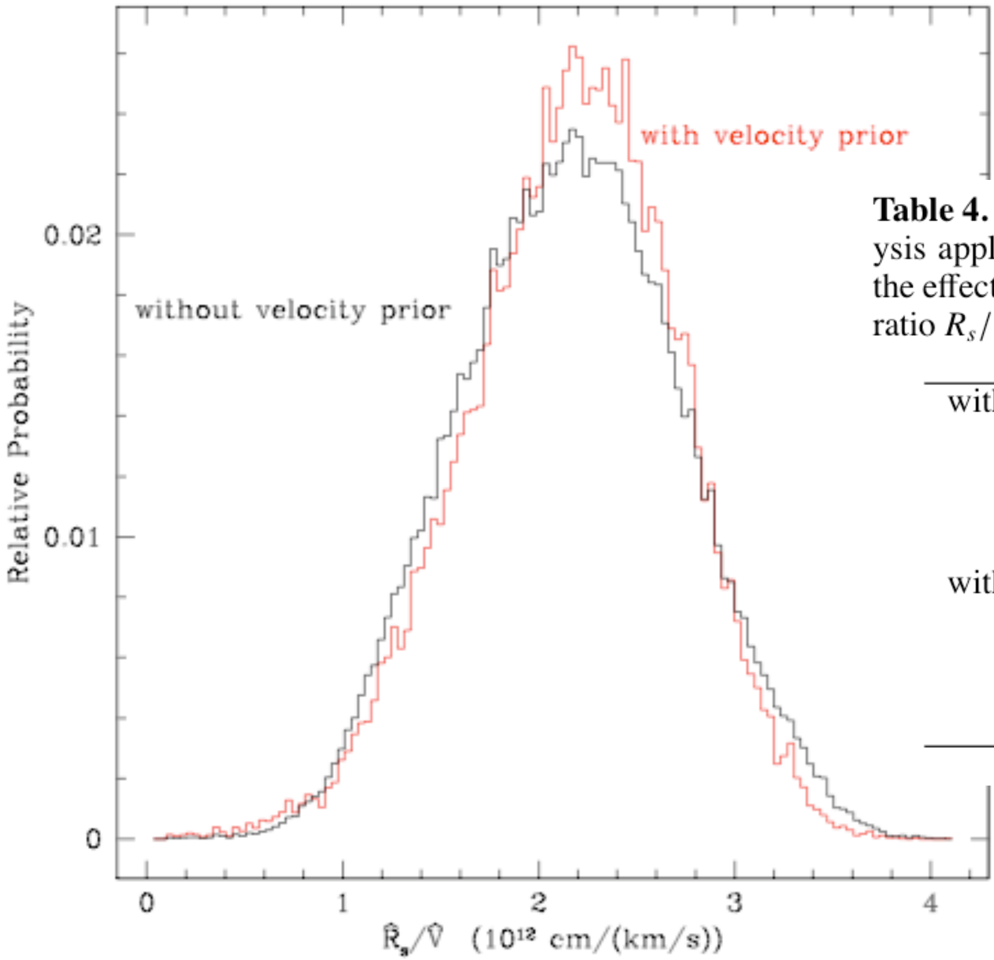

Table 4. Results from the microlensing simulations and Bayesian analysis applied to the OGLE data. We give the FWHM R_s of the source, the effective transverse velocity V measured in the source plane, and the ratio R_s/V.

with velocity prior	
	$\hat{R}_s = \left(9.2^{+6.9}_{-5.8}\right) \times 10^{15}\, \langle M/0.1 M_\odot \rangle^{1/2}$ cm $= \left(0.16^{+0.12}_{-0.10}\right)\, r_E$
	$\hat{V} = \left(3.9^{+3.0}_{-1.8}\right) \times 10^{3}\, \langle M/0.1 M_\odot \rangle^{1/2}$ km/s
	$\hat{R}_s/\hat{V} = (2.1 \pm 0.5) \times 10^{12}$ cm/(km/s)
without velocity prior	
	$\hat{R}_s = \left(4.0^{+7.5}_{-3.5}\right) \times 10^{16}\, \langle M/0.1 M_\odot \rangle^{1/2}$ cm $= \left(0.69^{+1.30}_{-0.60}\right)\, r_E$
	$\hat{V} = \left(1.8^{+2.8}_{-1.6}\right) \times 10^{4}\, \langle M/0.1 M_\odot \rangle^{1/2}$ km/s
	$\hat{R}_s/\hat{V} = (2.1 \pm 0.6) \times 10^{12}$ cm/(km/s)

Questions

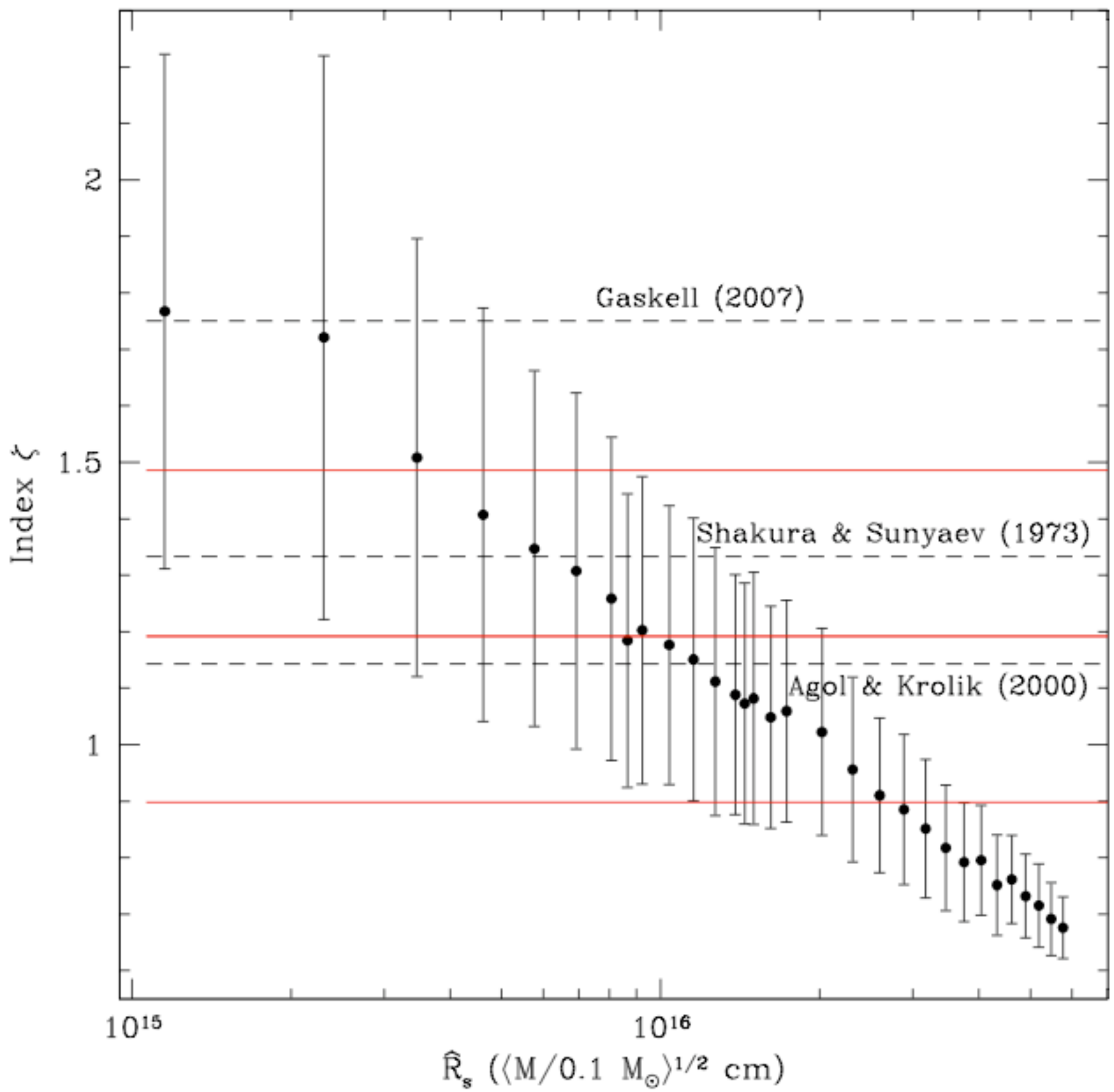

Gaskell (2007)
Shakura & Sunyaev (1973)
Agol & Krolik (2000)
Index ζ
2
1.5
1
10^{15}
10^{16}
$\hat{R}_s$ ($\langle M/0.1\ M_\odot \rangle^{1/2}$ cm)